

## Department of Precision and Microsystems Engineering

### Comparison of Photopolymer Resins for 3D Printing of Gradient Refractive Index (GRIN) Lenses

RUTWIK PATIL

Report no : 2024.072  
Coach : Dr. A. (Andres) Hunt  
Chair : Dr. N. (Nandini) Bhattacharya  
Specialisation : MECHATRONIC SYSTEM DESIGN  
Type of report : Msc Thesis Report  
Date : 27-08-2024

# Comparison of Photopolymer Resins for 3D Printing of Gradient Refractive Index (GRIN) Lenses

by

RUTWIK PATIL

Student Name	Student Number
Rutwik Patil	5813840

Committee:	Dr. Nandini Bhattacharya, Dr. Andres Hunt, Dr.ir. Sophinese Iskander-Rizk
Project Duration:	September, 2023 - August, 2024
Faculty:	Faculty of Mechanical Engineering, Delft



# Acknowledgement

The pursuit of a master's degree in mechanical engineering, specifically in High Tech Engineering Track, has been a life-changing experience whereby I have been able to acquire and develop various skills that are core in the discipline. A mix between theoretical learning and practical applications has remarkably formed my understanding and capability in mechanical engineering. Working on my thesis has fuelled my excitement and deepened my interest in the areas of optics and advanced materials. This experience has opened new avenues for exploration have proven very important for my professional growth.

First and foremost, I would like to thank my supervisors, Andres and Nandini, for their invaluable guidance, continuous support, and motivation throughout this research. Their expertise and insights have been instrumental in the completion of my thesis.

I am immensely thankful to my family back in India, who have always been my pillars of strength. Their love and belief vested in me despite the distance have been my greatest source of motivation. Hereby, I convey a special thanks to all my friends at home for going through all my phases during the thesis with me and constantly motivating me to keep going.

Moving ahead, special thanks to my friends here, who made this journey memorable with their support. Among these, I would like to specially mention to my "Haye-Tech" gang for being there for me (special shoutout to the necessary High-Tech parties). Their friendship and support have formed a big part of this experience; I thank them very much for all the fun, laughter, and teamwork that we shared. This journey would have been totally different without each one of you. Thank you all for your contribution to my success.

*RUTWIK PATIL  
Delft, August 2024*

# Abstract

This thesis aims to characterize the photopolymer resins designed for the 3D printing of Gradient Refractive Index (GRIN) lenses. This thesis focuses explicitly on preparing UV-curable inks doped with nanoparticles that are custom-synthesized for sophisticated optical applications. Four different ink formulations have been studied, including epoxy-based and PMMA-based, together with two commercial UV-curable resins, which are a combination of acrylates and epoxies. Spectroscopy testing of these inks is conducted to study their optical performance for properties like the transmittance and absorbance over the UV, visible light, and NIR regions. The results show that it is possible to obtain significantly different behavior in the optical properties of materials compared to the inks without nanoparticles, offering a promising pathway for developing GRIN lenses with superior characteristics. This research also reports on some modifications performed on an Elegoo Mars 4 DLP printer to control a projector and the DMD device for arbitrary exposure times, further contributing to the development of high-performance optical devices through additive manufacturing.

# Contents

<b>Preface</b>	<b>i</b>
<b>Abstract</b>	<b>ii</b>
<b>1 Introduction</b>	<b>1</b>
1.1 Background . . . . .	1
1.2 Motivation . . . . .	1
1.3 Scope . . . . .	1
1.4 Thesis Outline . . . . .	1
<b>2 Innovations in Multi-Material 3D Printing of GRIN Lenses</b>	<b>3</b>
2.1 Overview of GRIN Lenses . . . . .	3
2.2 Properties of Material used for 3D Printing of GRIN Lenses . . . . .	4
2.3 Multi-Material 3D Printing Techniques . . . . .	5
2.4 Multi-Material VAT Photopolymerization . . . . .	11
2.5 Advancements in Multi-Material DLP Printing . . . . .	12
2.6 Challenges in Multi-Material 3D Printing . . . . .	13
2.7 Summary . . . . .	13
<b>3 Adapting 3D Printer for GRIN Fabrication</b>	<b>14</b>
3.1 Description of the Elegoo Mars 4 DLP Printer . . . . .	14
3.2 Modification of DLP Printer . . . . .	14
3.2.1 Controlling the Digital Mirror Device . . . . .	15
3.3 Summary . . . . .	17
<b>4 Material Study</b>	<b>18</b>
4.1 Relevant Material Properties for Printing GRIN Lenses . . . . .	18
4.1.1 Selection of Base Polymers . . . . .	18
4.2 Components of UV Curable Inks . . . . .	20
4.2.1 Role of Photoinitiators . . . . .	20
4.2.2 Enhancing Material Properties with Additives . . . . .	21
4.3 Material Selection Criteria . . . . .	22
4.3.1 Selection of Monomer(s) . . . . .	22
4.3.2 Selection of Photoinitiator . . . . .	23
4.3.3 Selection of Additives . . . . .	23
4.4 Summary . . . . .	23
4.4.1 Base Monomer . . . . .	23
4.4.2 Photoinitiator . . . . .	23
4.4.3 Additives . . . . .	23
<b>5 Sample Preparation and Optical Measurements</b>	<b>25</b>
5.1 Preparation of Inks . . . . .	25
5.2 Formulation of Inks . . . . .	25
5.2.1 Preparation of Ink Samples . . . . .	25
5.3 Stoichiometry Calculations for Sample Preparations . . . . .	26

5.3.1	Stoichiometry Calculations for Epoxy Sample . . . . .	26
5.3.2	Stoichiometry for Ink Component Proportions for PMMA . . . . .	27
5.3.3	Stoichiometry for Ink Component Proportions for Anycubic Standard Clear Resin . . . . .	28
5.3.4	Preparation of Commercial UV Curable Resins . . . . .	28
5.4	Optical Performance Tests . . . . .	30
5.4.1	Ink Samples Prepared . . . . .	30
5.4.2	Spectroscopy Measurements Setup . . . . .	30
5.4.3	Measurement Procedure . . . . .	31
5.5	Refractive Index Study of Ink Samples . . . . .	31
5.5.1	Refractometry . . . . .	32
5.5.2	Ellipsometry . . . . .	33
<b>6</b>	<b>Results and Discussion</b>	<b>35</b>
6.1	Optical Properties of Prepared Samples . . . . .	35
6.1.1	Transmittance Comparison of Resins without Nanoparticles . . . . .	35
6.1.2	Transmittance Comparison of Resins with Nanoparticles . . . . .	36
6.1.3	Transmittance Comparison of Commercial UV Curable Resins . . . . .	37
6.1.4	Transmittance Results Comparison for Commercial Resins with Various Concentrations of Nanoparticles . . . . .	38
<b>7</b>	<b>Conclusion and Future Work</b>	<b>40</b>
7.0.1	Dispersion of ZrO <sub>2</sub> Nanoparticles . . . . .	40
7.0.2	Performance Comparison of DMPA Photoinitiator . . . . .	40
7.0.3	Curing Speed Comparison . . . . .	40
7.1	Optical Properties Analysis of Prepared Resin Samples . . . . .	40
7.2	Future Scope for Research . . . . .	41
<b>A</b>	<b>Appendix</b>	<b>46</b>
A.1	Materials Buy List . . . . .	48
A.2	Specifications of Elegoo Mars 4 DLP Printer . . . . .	49
A.2.1	Electronic Configuration of the Printer . . . . .	49
A.3	Individual Transmittance Results for Resins without Nanoparticles . . . . .	52
A.4	Individual Transmittance Results for Resins with Nanoparticles . . . . .	53
A.5	Transmittance and Absorbance Results in NIR Region for Resins with 0%wt ZrO <sub>2</sub> Nanoparticles . . . . .	54
A.6	Transmittance and Absorbance Results in NIR Region for Resins with 0.5%wt ZrO <sub>2</sub> Nanoparticles . . . . .	54
A.6.1	Transmittance Comparison of Resins with and without Nanoparticles for Each Resin . . . . .	55
A.7	Bill of Materials . . . . .	58

# Chapter 1

## Introduction

### 1.1 Background

For many years, the manufacturing of optical lenses has been done using traditional methods like grinding, molding, polishing, ion beam milling, and single diamond turning (SPDT). Each technique had disadvantages like high initial costs for mold fabrication and limitations in materials that can be used, like SPDT, for example, can only be used with soft plastics [1]. Even though advancements are made in these processes, they have some inherent drawbacks, like the material choices and surface quality. The recent innovations in advanced optical technologies are primarily based on creating complex materials and elaborate 3D printing methods. Innovation in this area happened with the introduction of Gradient Refractive Index (GRIN) lenses that allow a consistent change in refractive index within a lens, bringing many new possibilities in the transmission of light. A GRIN lens will improve optical performance by reducing aberrations, and at the same time, it facilitates the miniaturization of devices [2, 3, 4]. 3D printing through Digital Light Processing (DLP) promises an excellent route for fabricating such complex optical component devices where material properties can be controlled layer-by-layer. This thesis is dedicated to tailoring DLP three-dimensional printing technology to multi-material GRIN lens fabrication using nanoparticle-enhanced UV-curable inks.

### 1.2 Motivation

The motivation for this research arises from the need to develop advanced optical lenses that meet the demands of modern technology, particularly in fields such as telecommunications, medical imaging, and high-resolution microscopy [5, 6, 7]. The ability to fabricate GRIN lenses with high precision and tailored optical properties can lead to significant advancements in these areas. By leveraging the versatility of DLP 3D printing, this research aims to overcome the limitations of traditional manufacturing techniques, providing a scalable and efficient approach to producing high-performance GRIN lenses.

### 1.3 Scope

This thesis focuses on developing and characterizing UV-curable inks with nanoparticles, designed for 3D printing of GRIN lenses. The scope of the work includes formulating different ink compositions with nanoparticles, studying their characteristics, and finally customizing a DLP printer to handle these materials.

### 1.4 Thesis Outline

This thesis opens with a general overview of GRIN lenses and developments in multi-material 3D printing, with particular reference to the production of GRIN lenses in chapter 2. The description is followed by an

explanation of how the Digital Light Processing printer works and which specific modifications are made to enable it to implement the custom-designed printing approach used in this work in chapter 3. The detailed material study on the selection and characterization of base polymers, photoinitiators, and additives for the ink formulations in chapter 4. The inclusion of description of the experimental approach taken in preparing these ink samples, provides details on the stoichiometry behind the component proportions and the testing methodologies conducted to test the optical properties of the compositions. The results and discussions in chapter 6 analyze optical properties. Finally, when concluding the work in chapter 7, the thesis summarizes the most important findings and points for future research.

## Chapter 2

# Innovations in Multi-Material 3D Printing of GRIN Lenses

### 2.1 Overview of GRIN Lenses

Gradient Refractive Index (GRIN) lenses have a refractive index that varies continuously within the lens [8]. The refractive index in these lenses can be varied either axially (A-GRIN) or radially (R-GRIN) as shown in Figure 2.1 below.

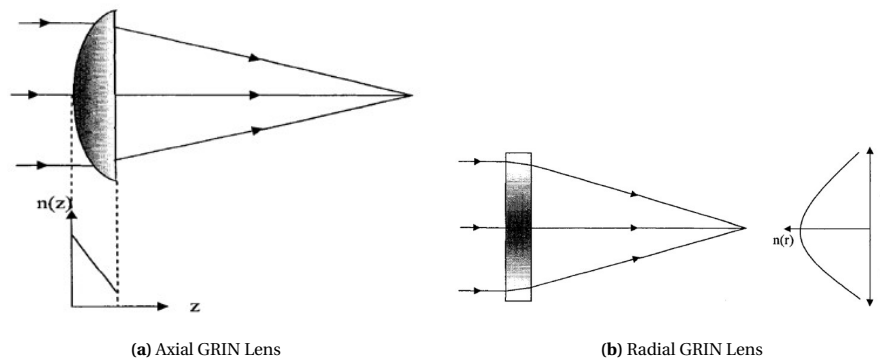


**Figure 2.1:** GRIN variation [9]

The fundamental difference between GRIN lenses and glass optics is the varying refractive index, this enables them to make the light behave in unique ways, reducing the aberrations present in the conventional lenses [10, 11, 12]. One of the main differences between both the types of lenses is that the focal length of the GRIN lens depends only on the thickness of the lens, whereas in the case of the conventional lens, it depends on both the radius of curvature and the thickness giving rise to the possibility of fabrication of flat GRIN lens. Due to this advantage, GRIN lenses have the capability to replace a multi-lens system makes the design of the complete optical system compact and lighter.

The focusing of the beam is due to the phenomenon of total internal reflection in contrast to the conventional lenses, where it's due to refraction only. As the refractive index varies in a radial GRIN lens varies continuously in  $y$ -direction, the rays experience constant refraction. Further refraction of the beam results in the beam reaching a critical angle, and hence, total internal reflection occurs.

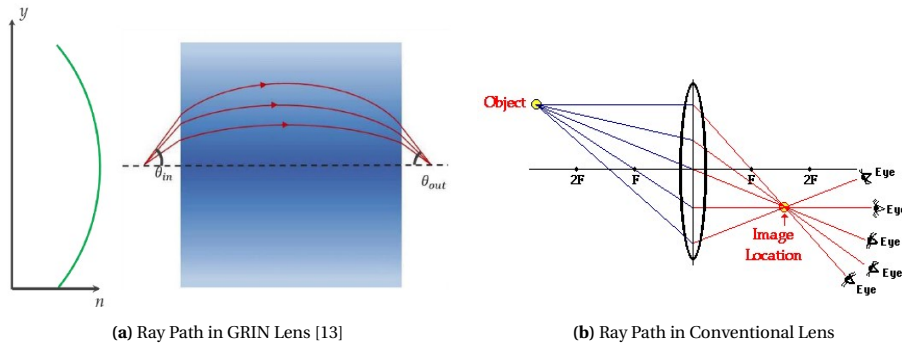


Figure 2.2: Ray Path Comparison

GRIN lenses are gaining importance in optical technology and are used in various fields like medical imaging for optical coherence tomography (OCT) because of their compact design [14]. They are also used in telecommunications to optimize signal transmission and accurately couple light efficiency between optical components. Compact high-resolution microscopy systems have also been developed with the help of GRIN lenses, which are used for biological research where imaging accuracy is of extreme importance [15].

## 2.2 Properties of Material used for 3D Printing of GRIN Lenses

Some properties of materials become more important and need to be considered when finalizing them for 3D printing of GRIN lenses. Following are those properties and why they play an important role:

**Optical clarity:** Materials with high optical clarity are desired in order to permit maximum light transmission by minimizing loss of light and ensuring the uniformity of transmitted light. Optical clarity also ensures that refraction of light is accurate which helps in reducing the aberrations and distortions in the final image eventually enhancing the imaging quality.

**Abbe number:** Abbe number primarily relates to minimizing aberrations and enhancing optical performance by reducing color spreading. Higher the abbe number lower is the dispersion property hence, materials with lower abbe number ensures that all the colors of white light focus closely increasing the sharpness of the obtained image.

**Surface Roughness:** Lenses ideally should have surface roughness less than 10nm [16]. Higher value of surface roughness can increase the scattering of light therefore reducing the efficiency of transmitted light and eventually affecting the contrast of the images. The 3D printing technology also affects the surface roughness of the product. Minimizing the surface roughness through material selection, printing method and post-processing techniques is therefore important [17].

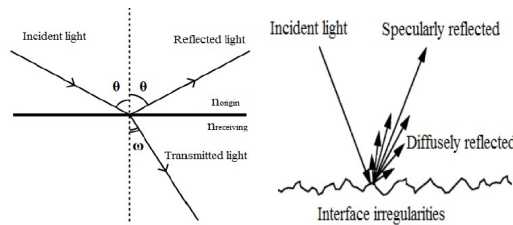
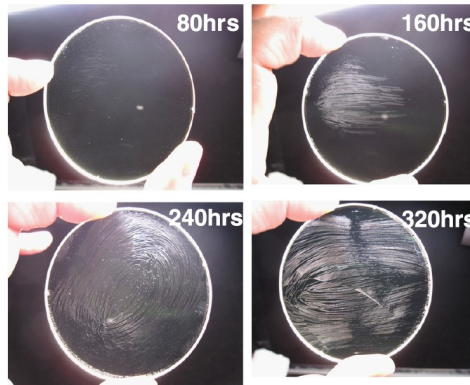


Figure 2.3: Figure shows light ray interaction with smooth surface (left) and and rough surface (right) of a lens

**UV Resistance:** As lenses will be subjected to UV light in their years of operation either from sunlight or artificial sources, it is necessary that they maintain their optical properties and dimensional stability over



time leading to a consistent long term performance. UV light also initiates chemical changes in the materials leading to brittleness and scratches on the surface of the lens [18]. The figure below shows an example how long-term UV exposure affect lenses fabricated by materials that aren't sufficiently UV resistant.



**Figure 2.4:** Lens coating failure under long-term exposure to UV radiation [18]

**Cross-linking:** The base polymer and the diluent used for viscosity have a major influence on this. The UV dosage is also a factor which control the cross-linking of polymers [19]. The photo-initiator concentration and the irradiation time also influence the cross-linking of the polymers as higher the photo-initiator concentration faster is the process and shorter is the irradiation time required.

**Viscosity:** The optimal viscosity of a material suitable for inkjet printing lies between 2-20mpa.s [16]. Materials with viscosity values higher than this can lead to clogging of the nozzles. Structural integrity and layer adhesion is also what gets affected due to viscosity of a material. Optimal viscosity ensures good adhesion between each layers which is crucial for structural integrity and mechanical properties of the final product.

Good control over refractive index gradients in the lens is also something which can be governed by viscosity as the refractive index gradient is achieved by varying the material composition or at times mixing multiple photopolymers. The viscosity of the materials hence ensures that this variation is consistent and precise to get an even distribution of refractive index throughout the lens.

**Geometric and Volumetric Shrinkage:** When dealing with photopolymers used for 3D printing, geometric and volumetric shrinkage plays a crucial role [20][21]. When the 3D printed object transitions from liquid to solid state it undergoes some dimensional changes. This change is known as geometric shrinkage. This property is usually influenced by the exposure time of the photopolymer to UV light and its chemical composition. The overall volumetric change in the printed object during the curing process is called the volumetric shrinkage. It is important to look into this property as this affects some crucial properties of the lens like its focal length. Volumetric shrinkage can also affect the gradient accuracy and for a GRIN lens precise gradient in the refractive index is important, any non-uniformity in this gradient will affect the final image quality.

## 2.3 Multi-Material 3D Printing Techniques

This gaining importance of GRIN lenses has led to advancements in their fabrication techniques. The methods used for their fabrication are mainly 3D printing techniques, as they help achieve precise control over a customized refractive index gradient and complex geometries desired for GRIN lenses. Work in additive manufacturing is done using various techniques like photopolymerization, direct laser writing, inkjet printing and digital light processing.

The fabrication of GRIN optics mainly involves mixing multiple materials. Since the refractive index and dispersion properties are closely linked, cross-linking of multiple optical polymers with different refractive

indices as 'inks' allows for a range of refractive index values which help optimize light transmission through the lens [16].

GRIN lenses fabrication needs accurate control over material properties to achieve the desired optical effects. Techniques like Stereolithography, Two-Photon Polymerization, and Direct Laser Writing are therefore most commonly used for their high resolution (around  $10\mu\text{m}$ ), precision, and versatility [16]. Here is a brief overview of how 3D printing of GRIN lenses is carried out by each technique:

### Multi - Material Aerosol Jet Printing

This method makes use of 2 different photopolymer liquids as the primary materials. These liquids are sprayed onto a substrate using an aerosol jet system, which allows for precise control of the layers' refractive indices by adjusting the photopolymers' mixing ratios. The pre-polymer layer is first applied to the already partially built structure. Then, this layer is selectively solidified using a UV laser, a crucial step in the process. The aerosol jet technique is particularly effective for applying liquid materials, as it evenly distributes the material over the substrate.

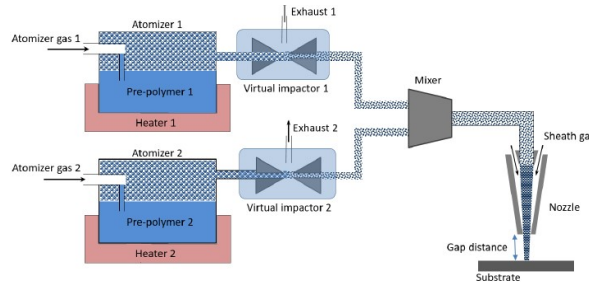


Figure 2.5: Lens fabricated by aerosol jet printing [16]

### Direct Laser Writing

Direct Laser Writing is a submicron level 3D printing technique that uses a femtosecond pulsed laser via a multiphoton polymerization process. Ocier et al. in their work presented a lithographic method in which they controlled the refractive index on a submicron level, creating voxels by varying beam exposure (SCRIBE) and achieved a GRIN lens with the refractive index of the lens varying from 1.85 to 1.28 for a 633nm light source [22].

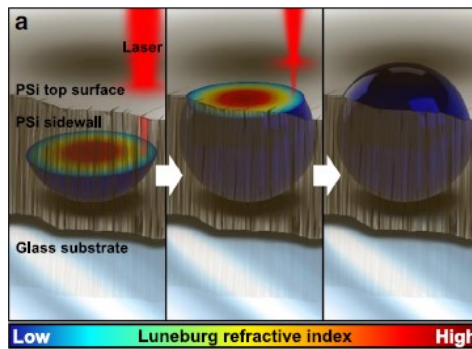


Figure 2.6: Spherical Luneburg lens printed inside Psi with SCRIBE [22]

### Inkjet Printing

The inkjet printing technique is modified to make it suitable for GRIN lens fabrication by using multiple print heads, each containing optical formulations of different indices of refraction in a layer-by-layer fashion. The central layer has the highest refractive index, with the refractive index decreasing as you leave the center in the case of a radial GRIN (R-GRIN) lens.

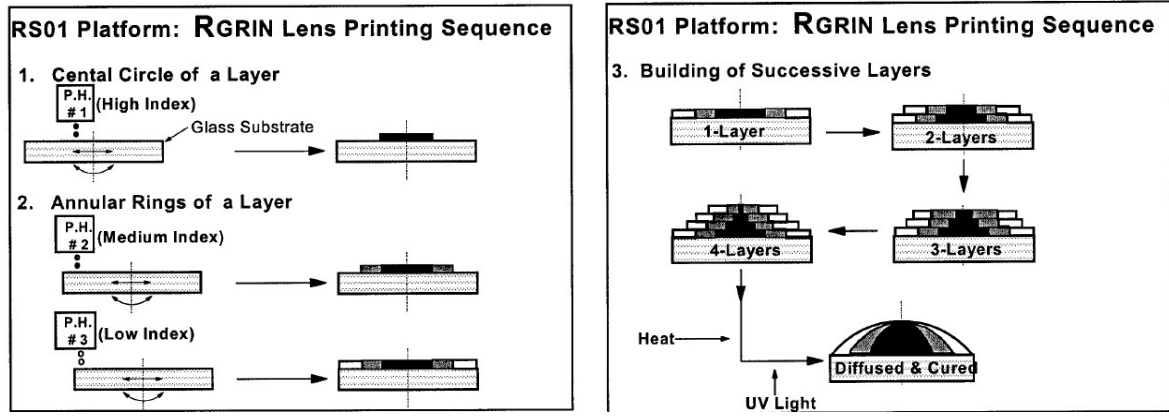


Figure 2.7: Inkjet printing of radial GRIN lens using 3 optical fluids [23]

### VAT Photopolymerization

VAT polymerization makes use of UV light and UV-curable resins. It involves stereolithography or Digital Light Processing (DLP), followed by post-processing to ensure uniformity in the fabricated lens. Stereolithography printers, in particular, are used to create optical lenses that are further refined for smoother surfaces, achieving a roughness as low as 6nm when using commercial glass molds [5, 19].

### Photopolymerization

Photopolymerization, especially Two-Photon Polymerization (2PP), is a key technique in manufacturing glass optics and GRIN lenses. This process can be applied in various ways. A flowchart depicting the classification of these photopolymerization techniques is shown in Figure 2.8.

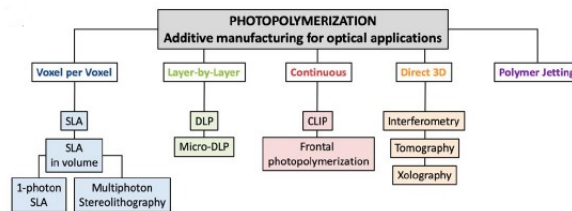


Figure 2.8: Main photopolymerization techniques [19]

Geisler et al. have discussed the progress in 3D printing of optics using photopolymerization, which indicates that lenses produced through layer-by-layer processes like DLP tend to have a higher resolution, in the order of  $5\mu\text{m}$ , compared to point-by-point methods [19]. However, these lenses often exhibit some stepped surface defects on their curved surfaces. These imperfections can be somewhat mitigated through thickness modulation techniques. The table below compares the commonly used 3 categories of photopolymerization techniques.

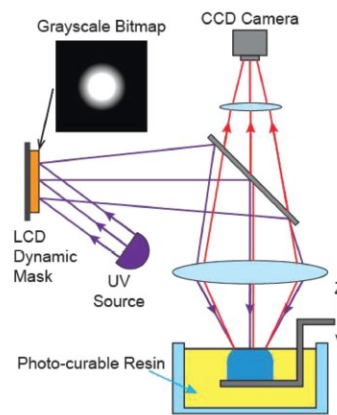
Categories	Advantages	Drawbacks
Point-by-Point Manufacturing (SLA)	Works with a range of photopolymer resins	Bulk and surface finish qualities don't meet the requirements
Layer-by-Layer (DLP)	Better surface finish compared to point-by-point methods	Gives rise to stepped surface defects on curved surfaces
Continuous Manufacturing Techniques	Eliminates material refilling steps like in SLA	Limited available resins due to viscosity considerations

Table 2.1: Comparison of Photopolymerization Techniques

Multi-material SLA printing involves using various photocurable resins to create intricate 3D objects with multiple colors or materials. This technique allows for integrating different materials in a single print, enabling the production of highly functional and complex structures. It typically includes a method to switch between materials and a cleaning process to prevent cross-contamination. The technology is advancing towards producing high-quality, multi-colored 3D models with minimal waste and improved precision. Maruyama et al., in their work, talk about a novel stereolithography system that utilizes multiple colored photocurable resins on a glass palette to create multicolor 3D models. The system features a translational stage for switching resins and a two-step cleaning process to prevent contamination [24].

### Digital Light Processing

Digital light processing is similar to SLA, except it uses light from an LED lamp in combination with a matrix of dynamic mirrors to cure the photopolymer resins. Unlike SLA, DLP illuminates the whole layer in one go, making this process relatively faster than SLA, although the lenses still exhibit stepped surface defects [19]. Chen et al., however, in their work, were able to fabricate a 3mm diameter and 5mm high aspherical lens with reduced defects with a resolution of  $5\mu\text{m}$  [25].



**Figure 2.9:** Digital light processing with post-processing steps [25]

### Hybrid Continuous Manufacturing Processes

Hybrid continuous manufacturing processes have also been developed, such as Continuous Liquid Interface Production (CLIP), Frontal Photopolymerization, and Light Assisted Polymer Jetting, which provide improved optical performance and reduce manufacturing time.

**CLIP Technology** is derived from Digital Light Processing (DLP) and is capable of generating objects continuously along the transverse axis. A key feature of CLIP technology is the management of a dead zone, also known as the light curing reaction inhibition zone, which is carefully controlled to ensure that a non-polymerized formulation of layers persists throughout the process. This inhibition zone can be achieved either through the action of molecular oxygen, as demonstrated by Tumbleston et al. [26], or by utilizing a photoinhibitor. In the latter case, a device that irradiates the resin with two distinct wavelengths is employed to maintain this zone effectively [27].

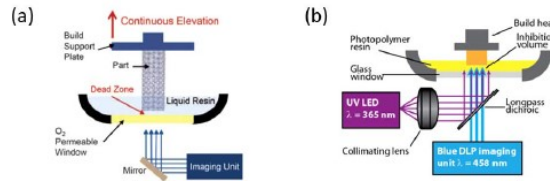


**Figure 2.10:** a) Schematic diagram of the CLIP technology [26]. b) schematic diagram of the CLIP technology with the photoinhibitor [27]

**Frontal Photopolymerization** involves the continuous propagation of a polymerization front with the assistance of a formulation that moves perpendicularly to the irradiated substrate. The heights cured are controlled by the light dosage from the light source. Typically, the absorbance of photoinitiators decreases during curing. However, if the resin either maintains or increases this absorbance during curing, the maximum achievable thickness is restricted. Frontal Photopolymerization is superior to CLIP technology in some aspects, as it can be programmed to control non-optical object deformation using techniques like origami.

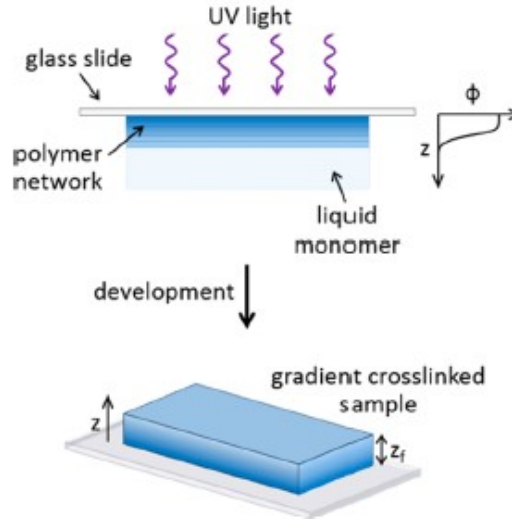


**Figure 2.11:** Frontal Photopolymerization [28]

**Light-Assisted Polymer Jetting** is another advanced fabrication technique, particularly useful for creating large optical elements with excellent surface quality. This process involves spraying micro-droplets of photopolymer resins onto the substrate, followed by immediate curing with an integrated UV laser source. The layers formed by this method are solidified instantly, ensuring precise control over the manufacturing process. Despite the capability to meet stringent requirements for optical elements, the performance of this method is still limited by the characteristics of the photopolymer resins used.

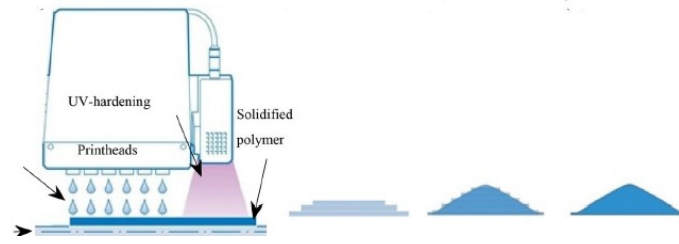


Figure 2.12: Light-Assisted Polymer Jetting [19]

### Voxel Based 3D Printing Techniques

A relatively recent development in the fabrication of GRIN lenses has been voxel-based fabrication techniques [29, 30]. Voxel-based techniques control the optical properties on a voxel level. A voxel is a volumetric pixel or a pixel in a 3D space. These techniques act on the subsurface level, therefore not affecting the surface of the lens, hence providing greater flexibility in terms of post-processing in comparison to traditional 3D printing techniques. Persembe et al., in their work, created a modified binder jetting technique using 360 dpi resolution piezoelectric printheads over 600 dpi thermal heads to overcome the limitations of a conventional setup [29].

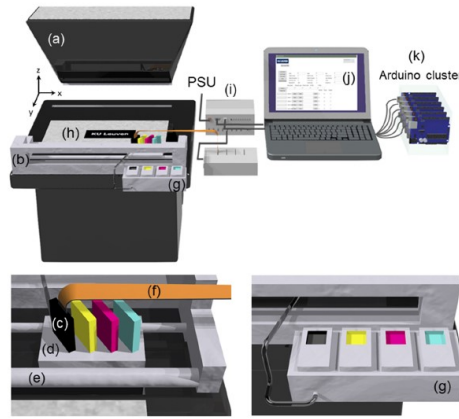


Figure 2.13: Schematic of customized binder jetting 3D printer [29]

A functionally graded material to demonstrate this voxel-based technique was printed as shown in the figure below.

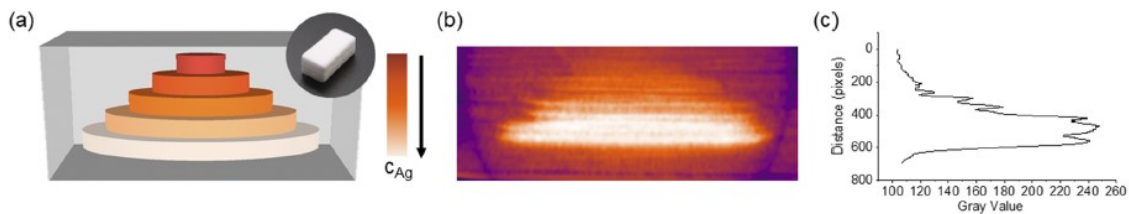


Figure 2.14: (a) CAD model of the object consisting of stacked disks. (b) Z-projection of the slices. (c) Gradient profile from the center of a projected slice in (b) [29]

This voxel level control over the optical properties was also achieved by Porte et al. in their work, where they managed to print optical components with a refractive index gradient of around 0.03 [30]. They achieved this by adding light exposure as an additional dimension to the traditional 3D laser writing. Using photoresists with exposure-dependent refractive index enabled them to print optical elements successfully. They performed this using a 780nm femtosecond pulsed laser with an average power of 20mW.



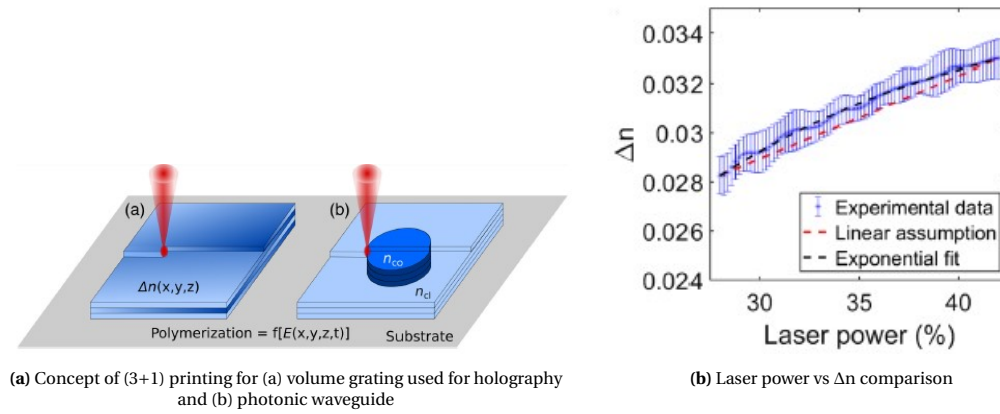


Figure 2.15: (3+1)D Printing working principle and result [30]

## 2.4 Multi-Material VAT Photopolymerization

As discussed in section 2.3 above, vat photopolymerization has various advantages but the technology is restricted by the material chemistries, design strategies and equipment limitations. The research community has made use of three primary strategies to successfully conduct 3D printing with the help of multi-material vat photopolymerization.

- Sequentially changing resins during 3D printing results in a multimaterial structure.
- During 3D printing, selectively activate photoreactions by changing the light source layer-by-layer for one resin formulation.
- 3D printing with a single resin formulation and selectively varying light intensity layer by layer.

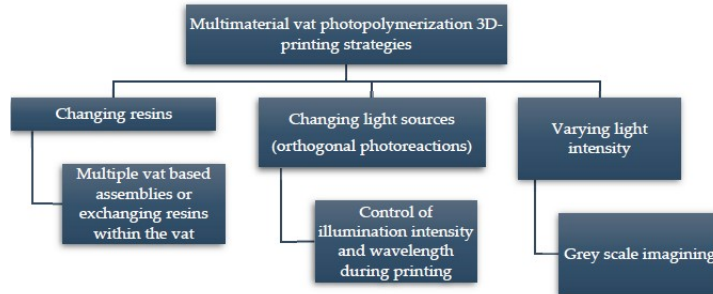


Figure 2.16: Multi-Material Vat Photopolymerization Strategies [31]

Most methods generally include mechanical or manual changing of vats or resins, but other techniques like dual-wavelength curing and varying light exposure. The Figure 2.17 below shows examples of manually and mechanically switching resins or resin vats Table A.1.

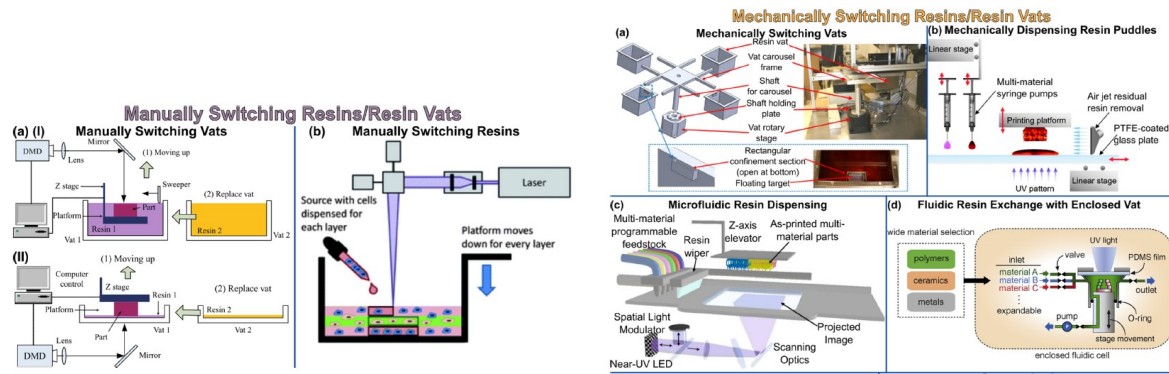


Figure 2.17: Manual and Hardware Multi-Material Vat Photopolymerization Approaches [32]

## 2.5 Advancements in Multi-Material DLP Printing

Hu et al., 2022 in their work describe the use of Digital Light Processing (DLP) for multi-ceramic additive manufacturing by developing a system that processes ceramic slurries with high viscosity through a cyclic method of "coating - exposure - cleaning - drying." Multiple ceramic slurries are stored in separate vats and exposed sequentially to UV light, allowing integration within a single layer [33].

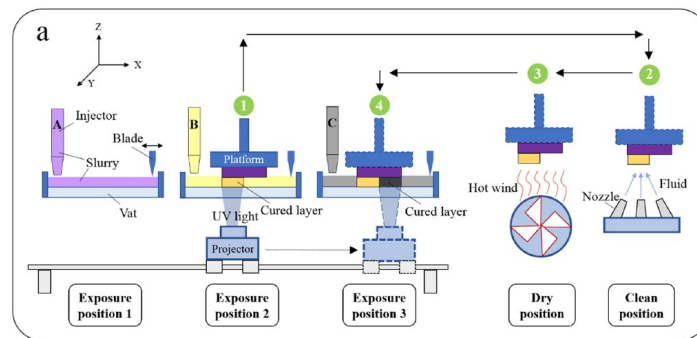


Figure 2.18: Multi-Ceramic DLP Printing [33]

The work done by Rossegger et al., 2023, involved multi-material DLP printing by synthesizing coumarin monomers with terminal acrylate functions using a dual-wavelength DLP printer [34]. Visible light (405nm) was used to polymerize the acrylate groups and UV-A light (365nm) to initiate coumarin dimerization. This enabled localised control over the mechanical properties and Tg. characterization which included FTIR, UV-Vis spectroscopy, DSC, and photorheology to confirm the photoreactions and assess the material properties.



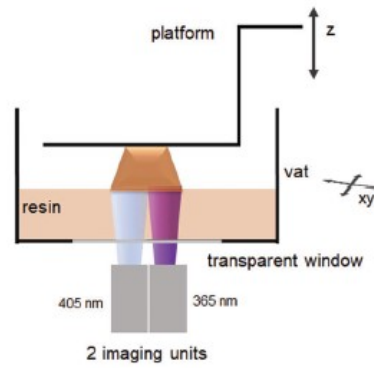


Figure 2.19: Multi-Material Dual Wavelength DLP Printing [34]

## 2.6 Challenges in Multi-Material 3D Printing

Multi-material DLP printing faces challenges, such as inter-stain in the intermediate layer of cured resins, and misalignment caused by multiple light sources or switching of vats. Researchers were able to perform multi-material 3D printing with the help of the vat photopolymerization techniques depicted in Figure 2.16, although the primary challenge in these techniques was the effective exchange and removal of the resin materials during the different printing steps. A large amount of work is done in these techniques by the top-down light scanning approach, where the platform is submerged into the resin vat, and the structure is printed along the z-axis. This approach gives rise to contamination and resin trapping within the confined areas of the sample.

Hence, the bottom-up approach is becoming fairly popular nowadays due to the minimum contact established between the building platform and the liquid resin, making the cleaning process of the materials and the printed sample much more convenient [35].

## 2.7 Summary

Digital Light Processing (DLP) is an emerging and highly effective technique for the 3D printing of multi-material lenses, particularly those with Gradient Refractive Index (GRIN). GRIN lenses feature a refractive index that varies within the lens, enabling distinctive light manipulation and minimizing aberrations compared to traditional lenses. The DLP process uses an LED light source and a dynamic mirror matrix to cure photopolymer resins. In contrast to stereolithography (SLA), which cures resin point-by-point, DLP cures entire layers at once, greatly increasing the printing speed. This technique allows for precise control over the lens's refractive index gradient and complex shapes, which is crucial for producing high-resolution optical components. While challenges such as stepped surface defects on curved surfaces exist, recent advancements have improved resolution to about  $5\mu\text{m}$ , establishing DLP as a quick and efficient method for fabricating intricate multi-material optical elements.

Digital Light Processing (DLP) stands out as an excellent choice for printing multi-material GRIN (Gradient Refractive Index) lenses due to several key advantages highlighted in the chapter:

- **High Resolution and Precision:** DLP offers high-resolution printing capabilities, which are extremely important for achieving precise control over refractive index gradients required for GRIN lenses.
- **Material Integration:** DLP is well-suited for multi-material printing, enabling the integration of different optical polymers with varying refractive indices within a single print.

## Chapter 3

# Adapting 3D Printer for GRIN Fabrication

### 3.1 Description of the Elegoo Mars 4 DLP Printer

For the work, Elegoo Mars 4 DLP printer® is the choice of the DLP printer due to its ease of use for customizing. The Elegoo Mars 4 DLP® is a desktop resin 3D printer that utilizes Digital Light Processing (DLP) technology, distinct from the more common LCD-based resin printers. This technology involves a digital projector that flashes an entire image of each layer at once, resulting in highly precise and uniform light curing.



**Figure 3.1:** Elegoo Mars 4 DLP Printer

### 3.2 Modification of DLP Printer

As discussed in section 2.5, the critical element for multi-material DLP printing is the varying exposure time according to the need of each of the resins used while printing, which is not possible without modifying the projector functioning algorithm as a DLP printer uses one fixed exposure time for one printing cycle. Hence, gaining complete control over the projector is important in the process.

The projector is connected to the controller board through I2C pins, which follow a two-wire serial communication protocol using a Serial Data Line (SDA) and a Serial Clock Line (SCL), which, in ideal cases, are connected from the projector controller board to the Power Supply Unit (PSU). So, an alternative is needed to configure these pins and gain control over them.

### 3.2.1 Controlling the Digital Mirror Device

Some approaches are tried to achieve control over the digital mirror device. First amongst them is to implement NanoDLP® custom software developed by Nano3DTEch [36]. NanoDLP® is a comprehensive software solution designed for controlling 3D prints on SLA, LCD, DLP and SLS printers. It acts both as a slicer and a controller to manage and control the printer's operation with the help of NanoDLP controller board.

Feature	Description
Slicing	Converts 3D models into 2D layers; supports adaptive thickness slicing.
Printer Control	Web-based interface for monitoring and controlling multiple printers in real-time.
Hardware Compatibility	Supports Raspberry Pi, Windows, Mac, and Linux; compatible with various hardware setups.
Advanced Features	Includes dynamic speed control, custom acceleration, resin usage estimation, multi-language support, and theme customization.
Additional Tools	NanoSupport for support generation; controller board for simplified printer setup.

**Table 3.1:** Key Features of NanoDLP

After the NanoDLP controller board is assembled, it has to be configured with a Raspberry Pi on which this board will act as a hat. To use the NanoDLP controller board, it needs to be wired to the following hardware inside the 3D printer:

- Stepper motor
- LCD Driver or Projector with HDMI connector
- Minimum endstop switch (NPN)

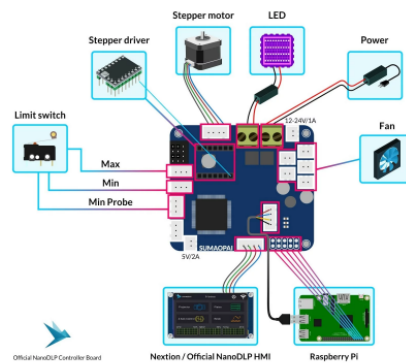


**Figure 3.2:** NanoDLP Controller Board Schematic

One of the main reasons that this method is not compatible with the Elegoo Mars 4 DLP printer since the projector in this printer is connected using two i2c pins instead of a HDMI connector. Hence, it is not possible to manage the projector without adding extra hardware to the NanoDLP controller board. Another reason that also restricts the functionality of this method is that even if integrating the controller board and Raspberry Pi with the printer is successful, the projector settings need to be controlled via the NanoDLP web-based slicing software only. Hence, not many customized commands can be given to the projector. This can be avoided if one is able to control the projector by running a Python script on the Raspberry Pi.

### OpenMLA PCB Design and Fabrication

It is possible to control the device by implementing a Python script on a Raspberry Pi and interfacing the Pi with the controller board. However, the controller board can't directly connect to the Raspberry Pi and an intermediate custom PCB is required. The reason for this is attributed to the DMD requiring a larger power input to switch on than the Raspberry Pi can supply, and the projector's controller requires real-time image processing and synchronization tasks like precise timing for the light source. Implementing this customization along with PCB design and fabrication is based on the repository [37].

The custom-made PCB integrates multiple components like the Raspberry Pi headers, JST SH 4-pin, and Molex PicoClasp connectors (12-pin and 8-pin), which are used to connect the i2c cables from the DLPC1438 controller board. A barrel jack for power input is also added. An additional Cui DC-DC converter and a  $100\mu\text{F}$  capacitor are added to convert the 12V supplied to the PCB to 5V to power the Raspberry Pi, so the Pi does not need to be powered separately. The Bill of Materials (BOM) can be found in Table A.5.

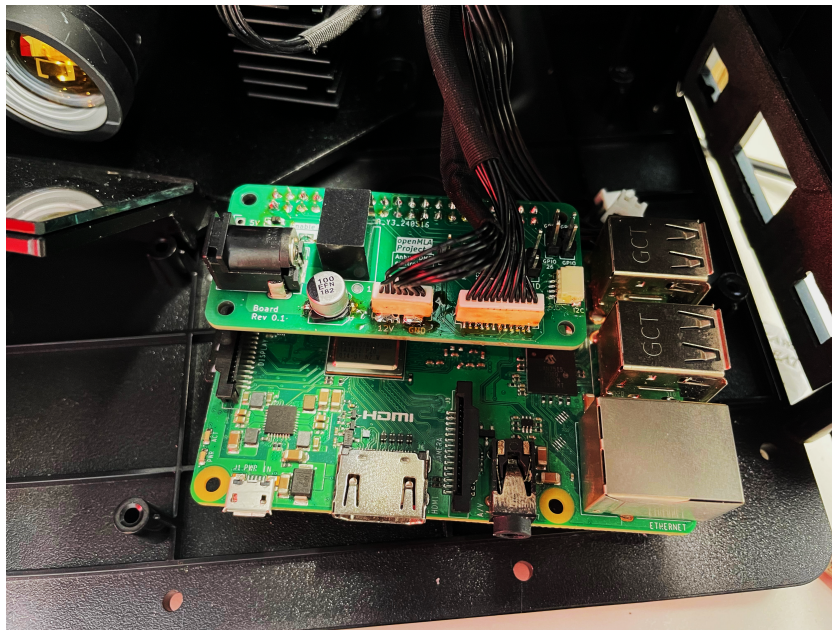
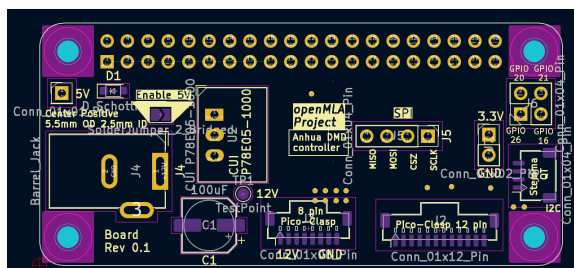
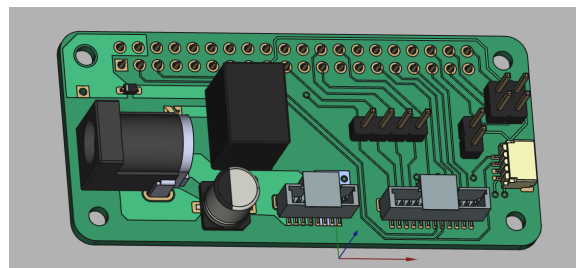


Figure 3.3: Assembled PCB and Raspberry Pi Setup

The board is designed in KiCAD 7.0® and fabricated by JLCPCB®. The complete functionality of the PCB can be found in [38].



(a) KiCAD Schematic of PCB



(b) Assembled PCB 3D Schematic View

Figure 3.4: Custom PCB Schematics [37]

### Raspberry Pi Configuration

After the custom PCB is fabricated, the next step is configuring the Raspberry Pi. A Raspberry Pi 3B+ is chosen on which the Raspbian OS 64-bit® is flashed. After configuring Wi-Fi and SSH on the pi to operate the pi

remotely, I2C and SPI interfaces are enabled using 'sudo raspi-config' and accessing the interfacing options menu. Finally, Python packages like 'smbus,' 'spider,' 'numpy,' and 'pillow' are installed.

Once the software setup for the Raspberry Pi is completed, a Python script found from the GitHub repository is run [37]. The aim is to switch the projector on and display multiple images, initially intermittently and then simultaneously as desired.

### 3.3 Summary

The main specifications of the Elegoo Mars 4 DLP printer are detailed in this chapter, its electronic configuration is described, and modifications necessary for multi-material printing are listed. The chosen printer is easily customizable and applies Digital Light Processing technology, which allows the curing of resin with the help of light. The necessary specifications include volumetric dimensions of the working area as 132.8 x 74.7 x 150 mm<sup>3</sup>, and the speed as **30-70 mm/h**. The chapter discusses the DLPC1438 3D print controller, which is the all-important glue to manage the DMDs and allows fine control of the printing parameters such as the layer exposure time and the LED current.

This is necessary because modifications to the printer are required which the standard setup does not allow. Hence, the required variable exposure times for different resins are not reached. The first trial is with the NanoDLP software and the respective controller board, but this proved incompatible because of the peculiar hardware setup of the Elegoo Mars 4. So, a custom PCB is designed and produced to be an interface between a Raspberry Pi and the printer's controller board for control through an executing Python script. This allows the printing process to be more flexible and accurate, including real-time image processing with projector synchronization.

## Chapter 4

# Material Study

### 4.1 Relevant Material Properties for Printing GRIN Lenses

Some material properties must be considered when printing lenses, affecting the final product's quality and performance [23]. The properties discussed in section 2.2 are summarized below in Table 4.1.

Property	Description
Optical Clarity	High optical clarity are desired so that the light passes without distortion
Abbe Number	A measure of material's dispersion. Higher the abbe number lower is the dispersion capability of the material
Surface Roughness	Surface of the material should allow smooth finishing to avoid imperfections affecting the performance of the lens
UV Resistance	Material shouldn't degrade significantly when in contact with UV light
Printability	Viscosity of the material should be such that it can be 3D printed easily
Cross-Linkability	The molecules in the inks used should form covalent bonds with each other
Geometric and Volumetric Shrinkage	This refers to shrinking of material after curing process affecting the properties of the optical lens fabricated

**Table 4.1:** Material properties summary

#### 4.1.1 Selection of Base Polymers

Optical materials generally consist of polymers, metals, ceramics, and nano-composites. However, polymers are the most widely used class of materials due to their variance in the refractive index (ranging from 1.3 to 1.7) and their reflectance being much lower than other materials as shown in Figure 4.1. Along with the wide range of refractive indices offered by polymers, they also offer outstanding optical clarity, and they also provide a range of viscosities as different 3D printing processes require different viscous inks for inkjet printing ( eg. 2-20MPa). In contrast, VAT polymerization techniques need lower viscosity ( 0.1 to 1 Pa) inks [16].

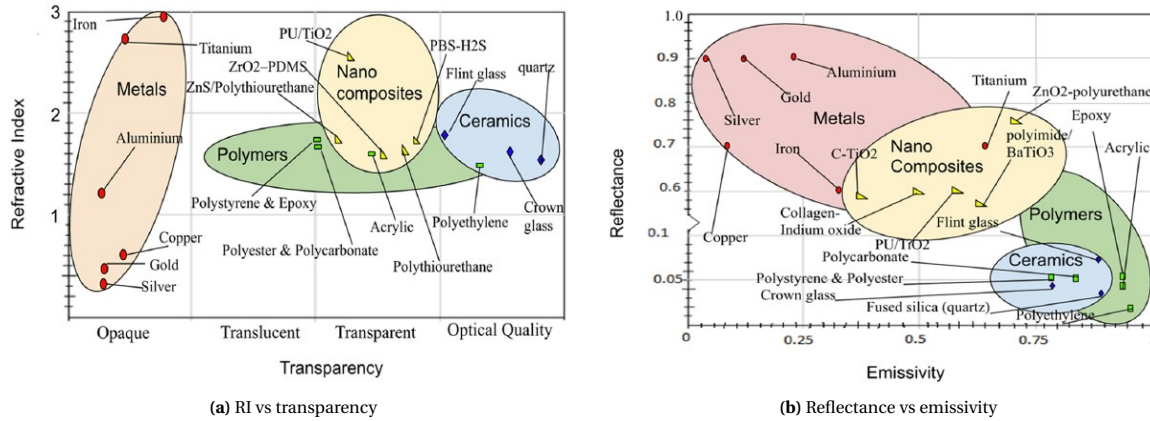


Figure 4.1: Material characteristics [10]

The materials used for 3D printing conventional and GRIN lenses are from the same family, polymers. However, GRIN lenses require a combination of multiple polymers along with some additives. The addition of zirconium dioxide nano-particles ( $ZrO_2$ ) to polymer resins, improves the cross-linking between the material and increases the refractive index value of the ink [39].

Since most multi-material 3D printing techniques, including DLP, involve UV curing, photopolymers are the best choice for the material [19]. The most widely used families of photopolymers are epoxies and acrylates due to their excellent optical clarity and ease of crosslinking with other additives like photoinitiators and nanoparticles, essential for achieving a tunable refractive index. Their ability to rapidly cure under UV light ensures high-resolution and accurate fabrication, which is crucial for optimum lens performance.

Three categories of resins are used for the 3D printing GRIN lenses: epoxies, non-UV formulated resins, commercial UV curable resins which are a mixture of acrylates and epoxides. A comparative study of these categories is depicted in detail in the section below. All three categories have significant differences in material properties. Those must be studied in detail before deciding what to use for the DLP printing.

Epoxy resin is a widely used adhesive product in various industries, including aerospace, automobile, marine, and civil engineering. Epoxy resins belong to the monomeric or oligomeric materials family and have excellent mechanical and chemical properties. The properties of epoxy resins depend on the combination of an epoxy resin and a curing agent. Tailoring cross-linkers and modifiers and selecting proper resins are critical to the steady growth rate of epoxy resins in various applications.

The commercial UV curable resins are a mixture of diacrylates and epoxide groups, are prepared with a photoinitiator that has been already mixed with them, making UV curing easier and faster than the remaining categories. On the other hand, epoxies and non-UV curable resins require a photoinitiator to make them curable by sources like UV light. A photoinitiator is a compound responsible for converting light energy into chemical energy to create a reactive molecule, which is done by photopolymerization.

Property	Acrylates	Epoxies
Optical Clarity	High transparency	Good optical clarity
Abbe Number	High Abbe number	Moderate Abbe number
UV Resistance	Excellent UV resistance	High UV resistance
3D Printability	Good 3D printability	Moderate 3D printability
Crosslinking	High crosslinking density	High crosslinking density
Geometric Shrinkage	Low geometric shrinkage	Moderate geometric shrinkage
Volumetric Shrinkage	Low volumetric shrinkage	Moderate volumetric shrinkage

Table 4.2: Acrylates vs Epoxy Material Property Comparison [40, 41]



## 4.2 Components of UV Curable Inks

UV curable inks consists of 3 components; the oligomers, photoinitiators and additives. Oligomer, being the base raw material in an ink, is present in maximum amount which undergo polymerization followed by cross-linking enabling the solidification process. Photoinitiators initiate the polymerization process of the monomers when subjected to UV radiation. Additives are added to the ink to enhance particular properties like the durability and viscosity. In the case of formulating inks for lens fabrication, additives are generally added to reduce the viscosity of the resin making it compatible with multiple processes like inkjet printing along with nanoparticles. This influences the light transmitting behaviour by modifying the refractive index of the material [42].

### Oligomer

Oligomers are elementary building blocks of the material, which link up to form a polymer. Depending on how they are solidified, there are 2 types of UV-curable inks: radical polymerization-based inks and cationic polymerization-based inks.

Feature	Free Radical Inks	Cationic Inks
Cure Speed	High	Moderate to high
Initiation	Light	Light or heat
Oxygen sensitivity	Yes	No
Shrinkage	Large	Negligible
Adhesion	Moderate to good	Excellent
Post Cure	Limited effect	Strong effect
Chemical resistance	Good	Moderate to good
Humidity resistance	No	Yes
Acid/base sensitivity	No	Yes

**Table 4.3:** Comparison between Radical and Cationic-Based UV Curable Inks

Epoxies come under the category of cationic inks which entitles that they have variety of good properties as listed in the table above over acrylates which are classified as free radical inks. Despite these advantages, epoxies are not widely used, mainly due to their low reactivity and high sensitivity towards environmental conditions like change in moisture or temperature. This makes them relatively less robust than acrylates [43].

To tackle this problem, one of the solutions is to use a resin, which is a mixture of an acrylate and an epoxy. This hybrid formulation is more reactive to polymerization and less susceptible to changes in environmental factors.

### 4.2.1 Role of Photoinitiators

Photoinitiators initiate Oligomer polymerization when in contact with UV radiation through cross-linking. The cross-linking process transforms the UV ink from a liquid to a solid state and fabricates the desired components layer-by-layer.



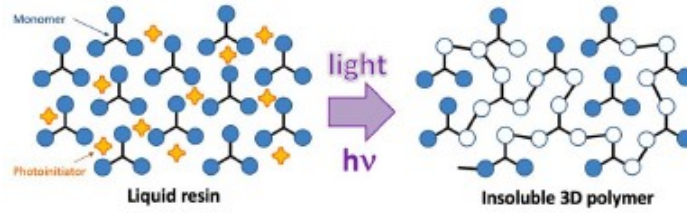


Figure 4.2: Schematic of Photopolymerization Process involving photoinitiator and Oligomer [19]

Epoxies' curing occurs through a polyaddition reaction in which the epoxy groups react with curing agents. In contrast, in the case of the non-UV curable resin prepared with PMMA, comes under the group of acrylates, they cure through a free radical polymerization mechanism. In this process, free radicals are generated using UV light, which propagates the polymerization reaction.

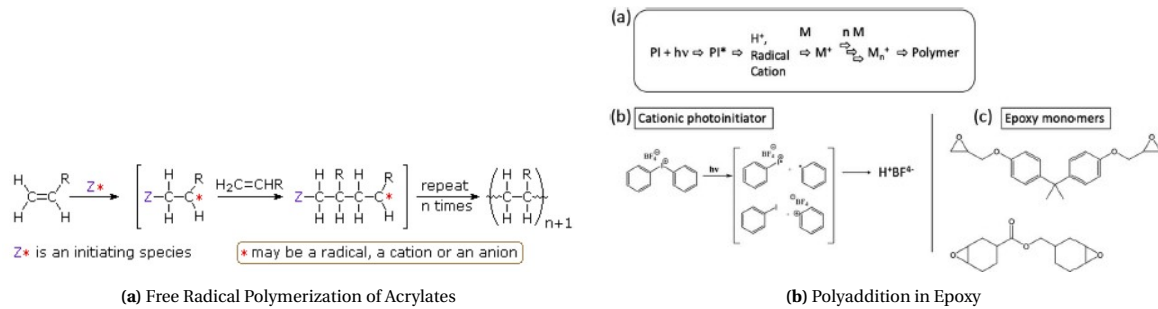


Figure 4.3: Different Polymerization Techniques [19]

### 4.2.2 Enhancing Material Properties with Additives

Various additives are added when preparing inks for 3D printing to enhance their mechanical properties. Mabrouk et al. increased the hardness and corrosion resistance of their 3D-printed scaffolds by adding titanium and aluminum alloys and various metal oxides [44]. Similarly, the optical properties of inks are also improved by dispersing nanoparticles in them.

Adding nanoparticles to inks for 3D printing optics enhances optical properties, such as the increased refractive index. It also enables the manufacturing multifunctional components, smart optics, and components with better surface quality.

#### Refractive Index Modification

GRIN lenses have various advantages in comparison to conventional optics as discussed in section 2.1. Control over the refractive index during resin formulation for DLP printing and, in turn, the refractive index of the fabricated lens is an important parameter. Several methods have been developed to alter the refractive index values of resin formulations. Gleissner et al. increased the refractive index of an epoxy acrylate polymer from 1.548 to 1.561 by adding phenanthrene in amounts from 0 to 15 wt% [45].

Another technique for altering the refractive index of resin formulations is the addition of inorganic nanoparticles into the inks, which are used to achieve higher refractive index. Zhang et al. used silicon nanoparticles to increase the refractive index of a siloxane-based polymer from 1.563 to 1.727 [46].

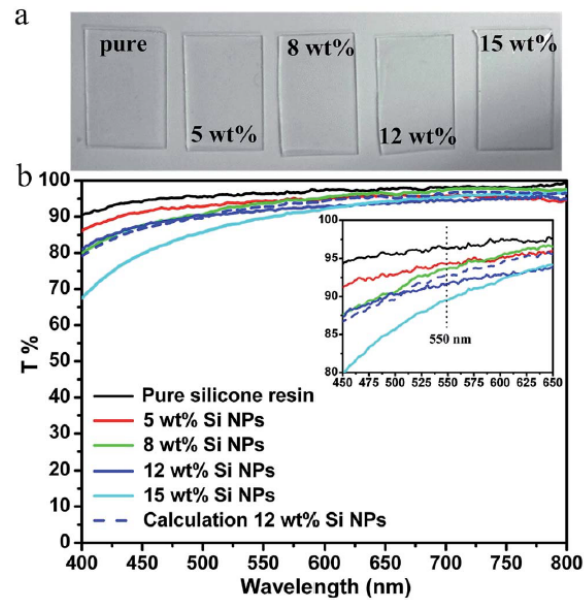


**Figure 4.4:** (a) Photographs of the obtained novel silicone hybrid films on glass substrates with different weight contents of Si NPs; (b) optical transmission spectra of these films [46]

### 4.3 Material Selection Criteria

After studying material categories, monomers, photoinitiators, and the role of additives in ink formulation, a choice has to be made for each of these components. It is important to accurately choose a suitable combination of all the 3 components in ink to achieve high-performance 3D printed lenses depicting excellent optical properties.

#### 4.3.1 Selection of Monomer(s)

UV ink formulations commonly make use of monofunctional or multifunctional acrylates. This is mainly due to their good resistance to hydrolysis, photo-stability and high transparency. Acrylate monomers also help in reducing the viscosity of the overall ink composition, making them also usable in Drop-on-Demand 3D printing methods.

While acrylate-based monomers remain the choice of material for these applications, epoxies are the second most widely used class of materials due to their good mechanical properties, relatively high thermal resistance and good optical properties [47].

Property	Monoacrylate	Diacrylate	Triacrylate	Tetraacrylate
Cure response	Slow	Moderate	Fast	Fastest
Flexibility	Very flexible	Flexible	Rigid	Brittle
Hardness	Softest	Moderate	Hard	Hardest
Solvent resistance	Low	Moderate	Good	Best
Adhesion	Good	Good	Moderate	Poor

**Table 4.4:** Comparison of properties for different acrylate types [16]

Along with purely organic monomers, the use of hybrid organic-inorganic resins as raw materials in UV ink formulations is also gaining more attention. Hybrid resins like ones having both acrylates and epoxide groups as base monomers provide several advantages like reduction in volumetric and geometric shrinkage, which is a prominent disadvantage in the case of acrylates, good optical performance, and relatively easy tuning of viscosity by the addition of an organic solvent like acetone [48].

### 4.3.2 Selection of Photoinitiator

A photoinitiator is a key element for every UV ink formulation. Photoinitiators are primarily classified depending on the mechanism of polymerization as mentioned in subsection 4.2.1. Benzoin derivatives like benzoin ethers were amongst the first to be employed for silicon-based monomers. However, they show inferior initiation with acrylate-based monomers. Benzyl ketone like 2, 2-dimethoxy-2-phenylacetophenone (DMPA) is a popular choice as they show good compatibility with acrylate based monomers, however they might be susceptible to yellowing in case of epoxies [49]. A list of these radical photoinitiators used in vat photopolymerization techniques can be found in Figure A.1.

### 4.3.3 Selection of Additives

As discussed previously in subsection 4.2.2, additives are used in UV ink formulations to enhance the existing properties of the final material. Nanoparticles are the primary choice of additives for enhancing optical properties of inks used for 3D printing of lenses to modify the refractive index of the material. Amongst the nanoparticles added to modify the refractive index, zirconium dioxide nanoparticles are proven to show an increase in the refractive index of the material along with maintaining high transmittance values of around 95% [50].

## 4.4 Summary

After studying the various material families and the components of UV curable inks, the following choices were made:

### 4.4.1 Base Monomer

- Epoxide Group Ink: This choice was made due to the good mechanical and chemical properties of epoxies, despite their sensitivity to environmental conditions.
- Acrylate PMMA Ink: Selected for its good resistance to hydrolysis, photo-stability, high transparency, and reduced viscosity, making it suitable for various printing methods.
- Hybrid Commercial Resins: A mixture of acrylate and epoxies was chosen to leverage the advantages of both materials, including reduced shrinkage and improved optical performance.

### 4.4.2 Photoinitiator

DMPA (2,2-Dimethoxy-2-phenylacetophenone): Chosen for its good compatibility with acrylate-based monomers and effective initiation of polymerization under UV light.

### 4.4.3 Additives

ZrO<sub>2</sub> (Zirconium Dioxide) Nanoparticles: Selected to enhance the refractive index and maintain high transmittance values, improving the optical properties of the final material.

These choices were made to ensure high-performance 3D printed lenses with excellent optical properties and mechanical stability. The image below summarizes the whole selection procedure.

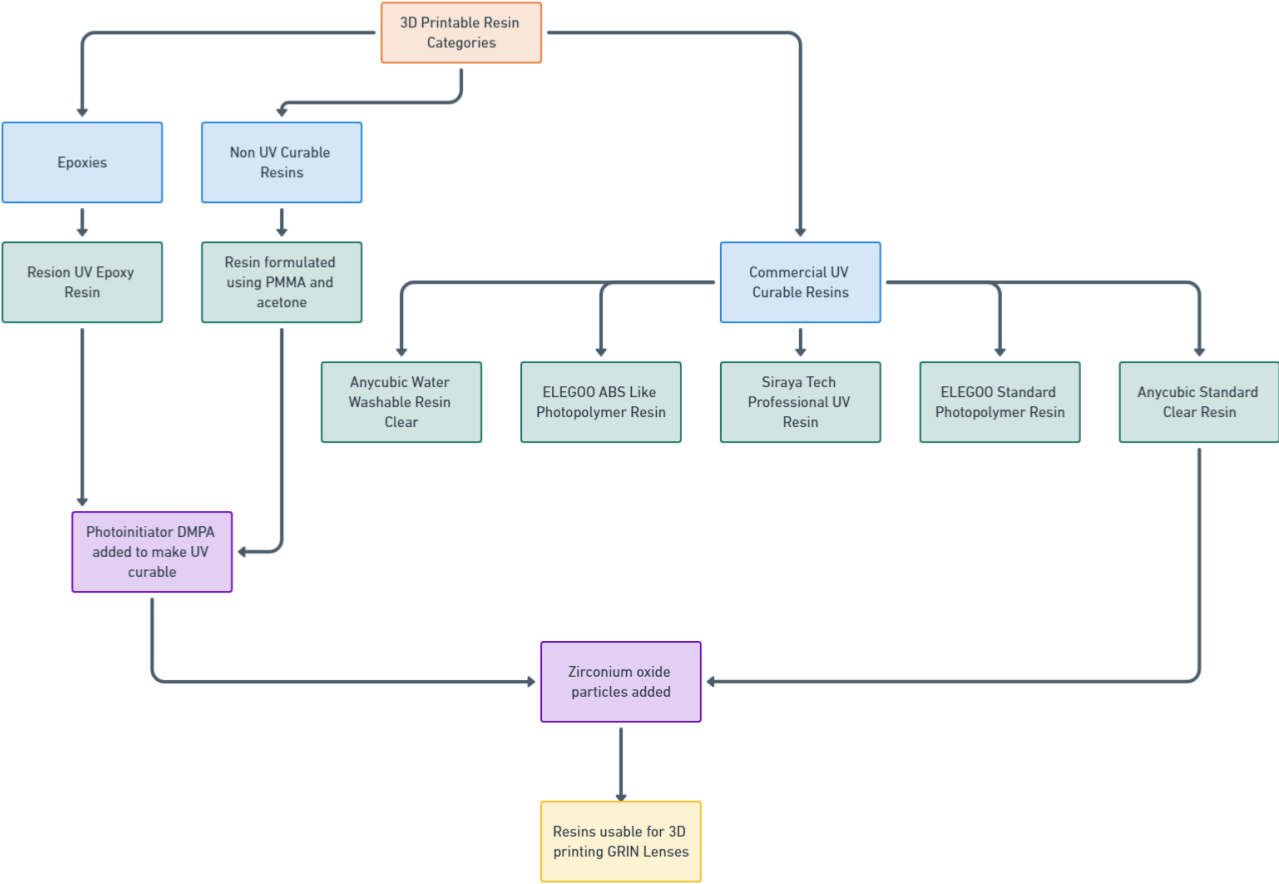


Figure 4.5: 3D Printable Resin Classification

## Chapter 5

# Sample Preparation and Optical Measurements

### 5.1 Preparation of Inks

After each of the components for ink formulation is finalized, three inks are prepared by carrying out various steps to get UV-curable inks suitable for DLP printing.

### 5.2 Formulation of Inks

Every ink formulation must undergo various stages to become a 3D printing resin compatible with a DLP printer like the ELegoo Mars 4 DLP used in this project. The three inks formulated have Resion Standard Clear Resin epoxy, PMMA, and Anycubic Standard Clear resin as the base monomer with DMPA as the photoinitiator and zirconium (IV) dioxide nanoparticles. Each of the three ink samples undergoes various steps to become a mixture of the monomer, the photoinitiator, and the nanoparticles. Initially, a 10ml sample of each of the inks is prepared.

#### 5.2.1 Preparation of Ink Samples

##### Mixing and Homogenization of Resion Epoxy with Nanoparticles solution and DMPA

The first step involves mixing 9 ml of the epoxy with 1 ml of Zirconium oxide nanoparticles solution. Since the nanoparticles were in a water solution and the epoxy was insoluble, phase separation in the mixture was observed when mixed using magnetic stirring or sonication. Therefore, the sample is kept in the oven at 110°C for 3 hours to evaporate the water.

After the water is evaporated, the nanoparticles remain suspended in the epoxy. Acetone is then added to the mixture to reduce the sample's viscosity and ensure the homogenization of the nanoparticles in the resin. The organic solvent acetone with the resin is mixed using magnetic stirring for 2 hours.

In the final step, before conducting UV curing of the sample, the DMPA photoinitiator must be added to make the ink curable. The white crystalline DMPA powder is in the sonication bath for 60 minutes. Finally, the mixture was homogenized using the Nanografi Homogenizer at 30% power for 10 minutes.

**Mixing and Homogenization of PMMA with Nanoparticles solution and DMPA**

The poly(methyl methacrylate) (PMMA) matrix is prepared with the incorporation of a photoinitiator, 2,2-dimethoxy-2-phenylacetophenone (DMPA), and zirconium oxide nanoparticles. Three Samples are prepared to have PMMA concentrations of 5%, 10%, and 15%, respectively. The quantity of the solution was kept constant at 10ml for all the samples. For the first step, the PMMA crystal powder is mixed in acetone.

After completion of this process, sedimentation in the sample containing 15% wt concentration of PMMA is observed, resulting in the solution turning milky. Since this wasn't observed in samples containing lower concentrations of PMMA, the sedimentation is a saturation of the solution due to a very high concentration of PMMA. As the rest of the samples show complete homogenized mixing, the sample having a 10% concentration of PMMA is selected for further preparations with the photoinitiator and nanoparticles.

For the addition of  $\text{ZrO}_2$  nanoparticles initially, similar steps as those for the epoxy sample are carried out. However, unlike epoxy resin, PMMA and acetone solutions have very low viscosity; hence, it isn't possible to directly add the nanoparticle solution to the PMMA and acetone mixture. So, the nanoparticle solution is kept in the oven to evaporate the water as much as possible to convert it into a paste, and then dilute the solution in acetone so that there is only one organic solvent, acetone, in the mixture. This mixing is done by continuous magnetic stirring for 2 hours.

The third step is mixing the white crystalline powder of the DMPA photoinitiator. The photoinitiator is remixed with the help of magnetic stirring until a homogenized clear solution is obtained. Finally, 1.5ml of this solution is pipetted into a cuvette and UV-cured for 1.5 hours. Three samples are prepared, UV-cured, and stored for upcoming spectroscopy measurements.

**Mixing and Homogenization of Anycubic Standard Resin(Clear) with Nanoparticles solution**

The Anycubic Standard Clear Resin is a hybrid resin that constitutes of 60% epoxy resins, 35% (1-methyl-1,2-ethanediyl)bis[oxy(methyl-2,1-ethanediyl)] diacrylate, and 5% of hydroxycyclohexyl phenyl ketone. 10ml of this resin and a small amount of acetone for adjusting viscosity are prepared using magnetic stirring. Since a diluted solution of  $\text{ZrO}_2$  and acetone is prepared in large amounts during the mixing and homogenization procedure for PMMA, the same solution is used to disperse nanoparticles even in this case. The nanoparticle solution is added to the resin and acetone mixture and mixed with the help of magnetic stirring for an hour. Since the Anycubic resin already has a photoinitiator present in it, mixing DMPA isn't necessary. So, after mixing the nanoparticles, 1.5ml of this sample is pipetted in a cuvette and UV-cured. Compared to the epoxy mixture, which took 3 hours to cure, and the PMMA mixture, which took more than an hour to cure, this Anycubic mixture completely cures in a minute, making the sample preparation much quicker than previous samples. Similar to previous cases, it is also stored for further spectroscopy tests.

**5.3 Stoichiometry Calculations for Sample Preparations**

All three components present in the ink need to be added in a specific amount to accurately predict or alter the properties of the final ink that is formulated, as having disproportionate amounts can have adverse effects on the optical performance of the fabricated product. This section shows these stoichiometry calculations of the samples.

**5.3.1 Stoichiometry Calculations for Epoxy Sample**

The intention is to make a 10ml solution containing epoxy resin, photoinitiator, and nanoparticles.

### Components and their Quantities

- **Resin**
  - Volume: 8 ml
- **Zirconium Dioxide (ZrO<sub>2</sub>) Nanoparticle Solution**
  - Original Concentration: 5% wt in 100 ml solution
  - Volume Added: 1 ml
  - Mass of ZrO<sub>2</sub> Nanoparticles in Original Solution:

$$\text{Mass of ZrO}_2 = \frac{5}{100} \times 100 \text{ g} = 5 \text{ g}$$

- Mass of ZrO<sub>2</sub> Nanoparticles in 1 ml Added:

$$\text{Mass of ZrO}_2 \text{ in 1 ml} = \frac{1}{100} \times 5 \text{ g} = 0.05 \text{ g}$$

- **DMPA Photoinitiator**
  - Mass: 0.1 g
- **Acetone**
  - Volume: Adjusted to fill the remaining volume to make up a total of 10 ml of the solution

A sample with similar proportions is also prepared where no nanoparticles are added, so it is a mixture of 8ml resin, 0.1g of DMPA, and 2ml of acetone.

Component	Amount	Percentage
Resin	8 ml	80%
Zirconium Dioxide (ZrO <sub>2</sub> ) Nanoparticles	0.05 g	0.5%
DMPA Photoinitiator	0.1 g	1%
Acetone	1.85ml	18.5%

**Table 5.1:** Components and Their Proportions in the 10 ml Epoxy Sample

### 5.3.2 Stoichiometry for Ink Component Proportions for PMMA

In the case of the sample with PMMA, as mentioned in subsection 5.2.1, three samples are prepared to have different concentrations of PMMA. The general formula for calculating the weight of PMMA ( $W_{\text{PMMA}}$ ) needed for a specific concentration is:

$$W_{\text{PMMA}} = \frac{C_{\text{PMMA}} \times W_{\text{acetone}}}{100 - C_{\text{PMMA}}}$$

#### Calculation for 5% PMMA Concentration in a 10ml Solution

- Desired PMMA concentration: 5%
- Weight of solvent (acetone): 7.6 g (10 ml of acetone)

$$W_{\text{PMMA}} = \frac{5 \times 7.6}{100 - 5} = \frac{5 \times 7.6}{95} = 0.4 \text{ g}$$

**Calculation for 10% PMMA Concentration in a 25ml Solution**

- Desired PMMA concentration: 10%
- Weight of solvent (acetone): 7.6 g ( 10ml of acetone)

$$W_{\text{PMMA}} = \frac{10 \times 7.6}{100 - 10} = \frac{10 \times 7.6}{90} = 0.844 \text{ g}$$

**Calculation for 15% PMMA Concentration in a 25ml Solution**

- Desired PMMA concentration: 15%
- Weight of solvent (acetone): 7.6 g ( 10ml of acetone)

$$W_{\text{PMMA}} = \frac{15 \times 7.6}{100 - 15} = \frac{15 \times 7.6}{85} = 1.341 \text{ g}$$

The proportions for the photoinitiator and nanoparticles is kept same as that for the epoxy sample. The table below summarizes these calculations.

Component	Amount for 5% PMMA	Amount for 10% PMMA	Amount for 15% PMMA
PMMA	0.4 g (5%)	0.844 g (10%)	1.341 g (15%)
Zirconium Dioxide (ZrO <sub>2</sub> ) Nanoparticles	0.05 g (0.5%)	0.05 g (0.5%)	0.05 g (0.5%)
DMPA Photoinitiator	0.1 g (1%)	0.1 g (1%)	0.1 g (1%)
Acetone	7.6 g (93.5%)	7.6 g (88.5%)	7.6 g (83.5%)

**Table 5.2:** Components and Their Proportions in 10ml PMMA Samples

**5.3.3 Stoichiometry for Ink Component Proportions for Anycubic Standard Clear Resin**

For this resin as addition of photoinitiator is not required only addition of nanoparticles is done which are added in same proportion as for previous samples.

Component	Amount	Percentage
Anycubic Standard Clear Resin	8 ml	80%
Zirconium Dioxide (ZrO <sub>2</sub> ) Nanoparticles	0.05 g	0.5%
Acetone	1.95ml	19.5%

**Table 5.3:** Components and Their Proportions in the 10 ml Anycubic Standard Clear Resin Sample

**5.3.4 Preparation of Commercial UV Curable Resins**

Along with preparing the inks with epoxy and acrylate, a set of cured samples of commercial UV curable resins are also prepared similar to Anycubic Standard Clear Resin as mentioned in subsection 5.2.1. Elegoo Standard Photopolymer Resin® , SIRAYA Tech Professional UV Resin® , Elegoo ABS-Like Photopolymer



Resin® , Anycubic Water-Wash Resin® are the materials selected. Each of the resins are a hybrid resin with combination of acrylates and epoxies. The tables below show composition of each of these resins.

Elegoo ABS Like Photopolymer Resin		
Component	CAS Number	Quantity (%)
Epoxy acrylate resin	61788-97-4	40-50
Monomer	13048-33-4	20-45
Color pigment	N/A	2-5
Photoinitiators	947-19-3	3-5
Elegoo Standard Photopolymer Resin		
Component	CAS Number	Quantity (%)
3,3,5-trimethylcyclohexyl acrylate	86178-38-3	53
4,4'-Isopropylidenediphenol, oligomeric reaction products with 1-chloro-2,3-epoxypropane, esters with acrylic acid	55818-57-0	26
(5-ethyl-1,3-dioxan-5-yl) methyl acrylate	66492-51-1	14
Ethyl phenyl(2,4,6-trimethylbenzoyl) phosphinate	84434-11-7	5
Titanium dioxide	13463-67-7	1.5
Anycubic Water-Wash Resin		
Component	CAS Number	Quantity (%)
Oxirane, 2-methyl-, polymer with oxirane, bis(2-methyl-2-propenoate)	122985-55-1	30 – 40
Polyethylene glycol diacrylate	26570-48-9	10 – 25
(1-methyl-1,2-ethanediyl)bis[oxy(methyl-2,1-ethanediyl)] diacrylate	42978-66-5	15 – 25
Poly(oxy-1,2-ethanediyl), .alpha.,.alpha. '-[(1-methylethylidene)di-4,1-phenylene] bis [.omega.-[(1-oxo-2-propen-1-yl)oxy]	64401-02-1	10 – 20
Phenyl bis (2,4,6-trimethylbenzoyl)-phosphine oxide	162881-26-7	2 – 5
Anycubic Standard Clear Resin		
Component	CAS Number	Quantity (%)
Epoxy resins	61788-97-4	60
(1-methyl-1,2-ethanediyl)bis[{}oxy(methyl-2,1-ethanediyl){}] diacrylate	42978-66-5	35
Hydroxycyclohexyl phenyl ketone	947-19-3	5
Siraya Tech Professional UV Resin		
Component	CAS Number	Quantity (%)
Urethane Acrylate	877072-28-1	35-65
Acrylic Monomer	64401-02-1	25-40
Photoinitiator	119-61-9	0-5

**Table 5.4:** Composition of Commercial UV Curable Resins [51, 52, 53, 54]

## 5.4 Optical Performance Tests

After the samples of all three inks are cured, optical performance tests are conducted on them. In case of lenses, transmittance is one of the key property along with refractive index that needs to be studied. Hence, the transmittance of these samples is measured. An Avantes AvaSpec® spectrometer and Avantes Avalight® deuterium and halogen light source is used to conduct the spectroscopy measurements.

### 5.4.1 Ink Samples Prepared

In this study, a series of ink samples are prepared with varying concentrations of  $\text{ZrO}_2$  nanoparticles. Specifically, Resion UV Epoxy, PMMA, Anycubic Standard Clear Resin, and Elegoo Standard Photopolymer Resin are each formulated with and without 0.5% wt  $\text{ZrO}_2$  nanoparticles to investigate the effects of nanoparticle inclusion on the material properties as described in section 5.3.

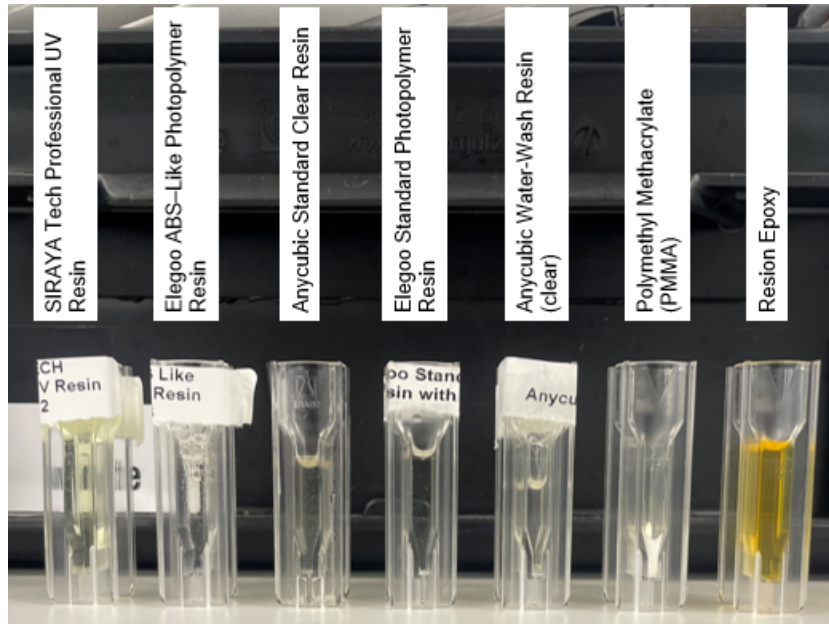
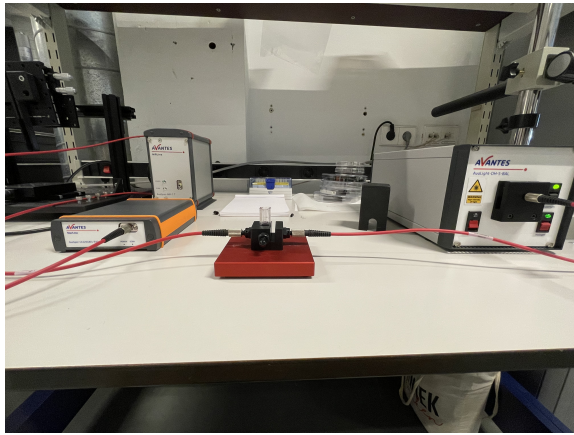


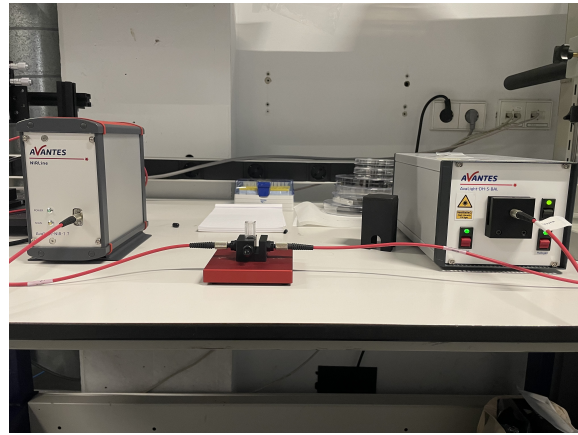
**Figure 5.1:** Prepared Photopolymer Resin Samples with 0.5%  $\text{ZrO}_2$  Nanoparticles

### 5.4.2 Spectroscopy Measurements Setup

The spectroscopy measurements for transmittance and absorbance are conducted using the Avantes UV and Visible Light Spectrometer and the AvaSpec-NIR256/512-1.7-EVO NIR Spectrometer, covering the UV, visible, and near-infrared (NIR) regions. The light source utilized in these measurements is the Avantes Deuterium and Halogen Light Source, which is allowed to heat up for 20-30 minutes to ensure stable output. For the measurement setup, the spectrometers and light source are connected to the cuvette holder and finally the measurements are conducted and recorded on the Avantes Avasoft 8 software.



(a) Spectroscopy Setup for UV-VIS Spectrometer

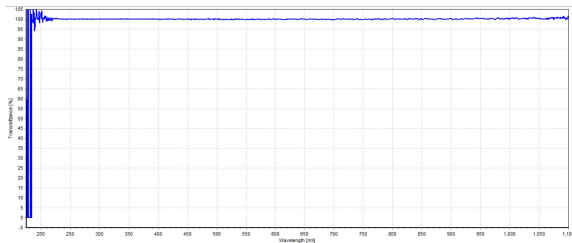


(b) Spectroscopy Setup for NIR Spectrometer

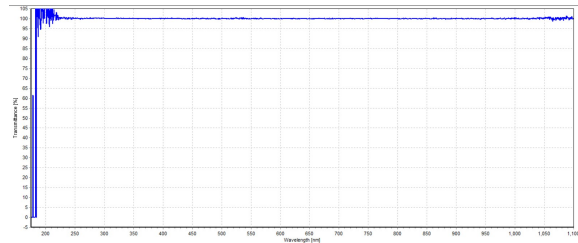
**Figure 5.2:** Spectroscopy Measurement Setup

### 5.4.3 Measurement Procedure

To ensure accurate transmittance readings, the process begins with setting up reference readings using the Avasoft software. In order to take transmittance readings, it is necessary to take accurate reference readings. Hence, it is necessary to take reference readings both with an empty cuvette and without a cuvette for baseline correction. Readings taken without a cuvette in the holder accounts for any inherent noise or background signal in the system including reflections, scatter, and electronic noise. This ensures that the measurement taken only reflects sample's effect on the light and not the system's inherent characteristics. Whereas, when you take a reference reading with an empty cuvette, you can correct the optical characteristics of the cuvette. However, as the Figure 5.3 shows, both the measurements are close to each other except for the noise which is observed until 250nm wavelength, which ensures that the measurements taken with a cuvette containing a sample shows optical characteristics of only the sample. The reference reading with an empty cuvette is then taken by placing the cuvette in the cuvette holder, then the shutter is switched on and a bright reference reading is taken. Afterwards, by switching the shutter off a dark reference reading is taken.



(a) Reference Reading Without a Cuvette



(b) Reference Reading with an Empty Cuvette

**Figure 5.3:** Reference Reading Comparison

These reference readings, which account for both the inherent noise of the system and the optical characteristics of the cuvette, are then set in the Avasoft software to establish a baseline. After the reference readings are correctly established, the system is switched to transmittance mode, where the transmittance should read 100% with the empty cuvette in place. Following this, the empty cuvette is replaced with a cuvette containing the cured sample, and the transmittance plots are observed and recorded. This procedure is repeated for each of the prepared ink samples to ensure consistent and accurate measurements of their optical properties.

## 5.5 Refractive Index Study of Ink Samples

Integration of  $\text{ZrO}_2$  nanoparticles to resin formulations for DLP 3D printing increases the sample's refractive index as mentioned in subsection 4.3.3. Since it is a crucial property when studying the transmission of light

through a material, it is essential to study the change in the material's refractive index. Some of the methods used measure the refractive index of a sample are ellipsometry and refractometry [55, 56].

### 5.5.1 Refractometry

When a light ray in air is incident at an angle  $\theta_i$  on one side of the prism with refractive index  $n_1$  and base angle  $\theta_p$ . The light ray is refracted into the prism and it propagates towards the bottom surface of the prism. There is a boundary between the bottom surface and the test resin sample of refractive index  $n_2$ , where  $n_1 > n_2$ . If the incidence angle at the boundary is  $\theta_1$  we have:

$$\theta_1 = \theta_p + \sin^{-1} \left( \frac{\sin \theta_i}{n_1} \right) \quad (5.1)$$

The phase difference of  $s$  polarization relative to  $p$  polarization as explained by Fresnel's equations is given by:

$$\phi = \delta_s - \delta_p = 2 \tan^{-1} \left[ \frac{(\sin^2 \theta_1 - n^2)^{1/2}}{\tan \theta_1 \sin \theta_1} \right] \quad (5.2)$$

where  $n = n_2 / n_1$

Substituting Equation 5.1 into Equation 5.2 we get:

$$n = \sin \left[ \theta_p + \sin^{-1} \left( \frac{\sin \theta_i}{n_1} \right) \right] \times \left\{ 1 - \tan^2 \left( \frac{\phi}{2} \right) \tan^2 \left[ \theta_p + \sin^{-1} \left( \frac{\sin \theta_i}{n_1} \right) \right] \right\}^{1/2} \quad (5.3)$$

From Equation 5.3,  $n_2$  can be calculated by measuring the phase difference  $\phi$  under experimental conditions in which values for  $\theta_i$ ,  $\theta_p$  and  $n_1$  are given.

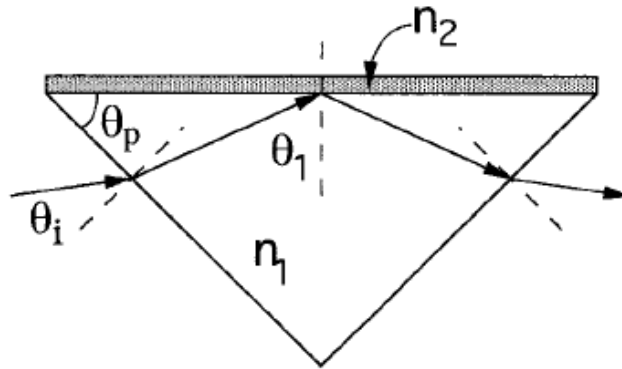


**Figure 5.4:** Total internal reflection at the boundary between a prism and a test sample [57]

However, refractometry can only be used assuming that the material is isotropic after homogeneous dispersion of  $\text{ZrO}_2$  nanoparticles hence having uniform refractive index. Non-homogeneous dispersion of nanoparticles can lead to making the material anisotropic giving rise to birefringence. This birefringence results in splitting of light beam into ordinary ray (o-ray) and extraordinary ray (e-ray), each travelling at different speeds refracting at different angles. In case of anisotropic materials, ellipsometry can be used for measurement of refractive index. Another assumption that is made is that the value of refractive index of air is 1.0. However, that is untrue as it is heavily dependent on the environmental conditions like temperature, humidity and atmospheric pressure. The dependence of refractive index on these conditions is given by Edlen's equation given below.

$$n - 1 = (n_0 - 1)(96095.43P) \left( 1 + f(0.0000624 - 0.00001358T) + 0.0036610(T - 273.15) \right) \quad (5.4)$$

where,

$T$  = Temperature in Kelvin

$P$  = Pressure in Pascals

$f$  = Correction Factor

### 5.5.2 Ellipsometry

Ellipsometry measures the change in polarization of reflected light from a material surface. When the light wave reflects off the surface, the linear polarization changes to elliptical polarization. This means that the amplitude and mutual phase of the p and s component of  $E$  changes causing the endpoint of  $E$  to move into an ellipse. It analyses the change in polarization of light for the o-ray and e-ray in birefringent materials, measuring different values of refractive indices ( $n_o$  and  $n_e$ ).

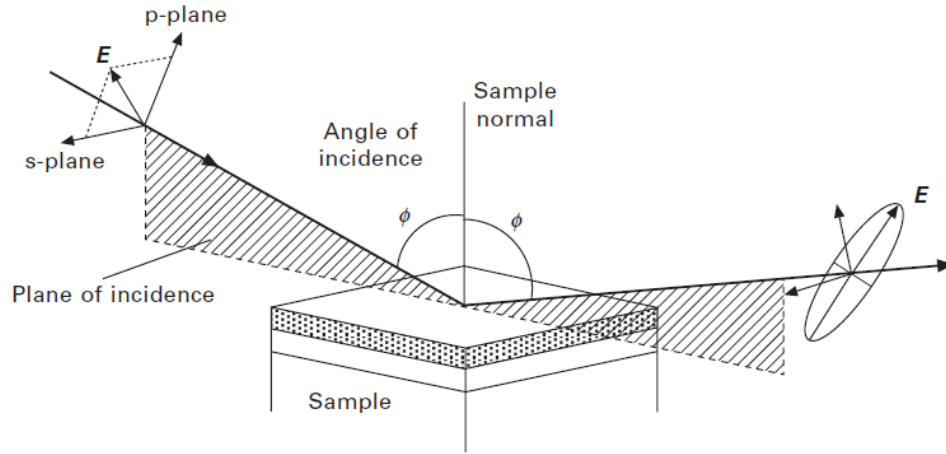


Figure 5.5: Ellipsometry Working Principle [55]

The ellipsometric parameters that being the reflection coefficients of light polarized parallel and perpendicular to the plane of incidence  $R_p$  and  $R_s$  respectively. The Equation 5.5 shows this relation of these two reflection coefficients.

$$\rho = R_p/R_s = \tan(\psi)e^{i\Delta} \quad (5.5)$$

where

$\Psi$  = ratio of reflected amplitudes  $\Delta$  = phase difference after reflection

Ellipsometry is generally used to measure thickness of thin films on top of a substrate, glass for example. The Figure 5.6 below shows a simplified model of this. if the refractive indices of the thin film and substrate is known, it is possible to calculate thickness of the film by ellipsometry.

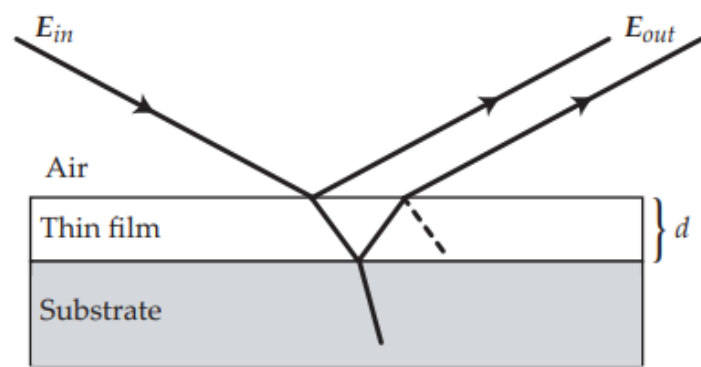


**Figure 5.6:** Illustration of Thin Film on top of a Crystal [58]

## Chapter 6

# Results and Discussion

### 6.1 Optical Properties of Prepared Samples

As discussed in chapter 5, during the preparation of the three samples, various findings are observed in multiple aspects like dispersion of nanoparticles, photoinitiator performance difference for epoxies and acrylates, and curing speed variation. The effect due to each of this change can be seen in the transmittance plots.

#### 6.1.1 Transmittance Comparison of Resins without Nanoparticles

As seen in Figure 6.1, the transmittance of epoxy sample increases with wavelength. The transmittance remains near zero until the wavelength of around 405nm when the photoinitiator starts to act and cure the sample. Hence, after 405nm, the transmittance starts increasing rapidly and crosses the value of 80% at 600nm wavelength. The resin absorbs most of the light at shorter wavelengths (<400nm), resulting in a low transmittance value. The plot for the Anycubic Standard Clear resin also shows similar trends where there is a rapid increase in the transmittance around 400nm, and above 50, it becomes highly transparent with transmittance values reaching 90%. In the case of the PMMA Sample without nanoparticles, the transmittance suddenly increases at a much lower wavelength (320nm). It has already crossed the value of 90% before 600nm wavelength and remains above 95% for the rest of the wavelength.

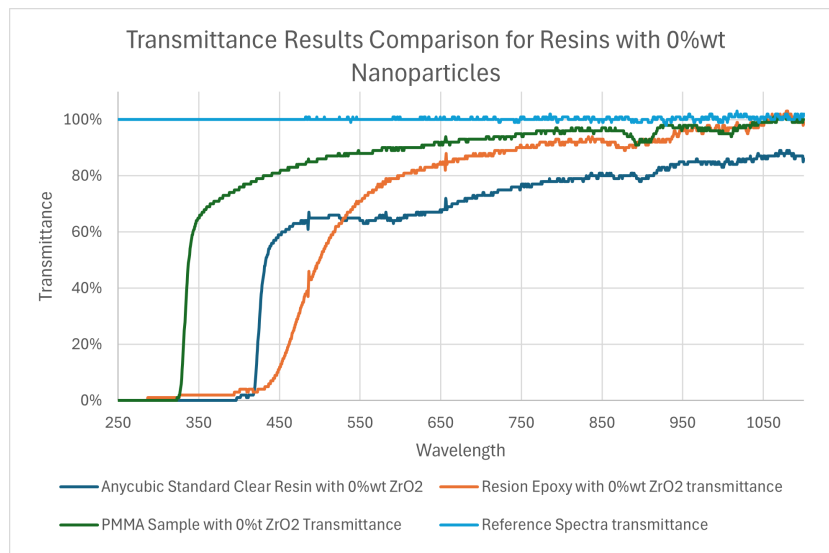


**Figure 6.1:** Transmittance Comparison of Resins without Nanoparticles

In near-infrared region (NIR), each of the resins show a similar trend with notable dips in transmittance around 1200nm, 1400nm, and 1650nm wavelengths, where PMMA shows the highest average transmittance of 80% followed by Resion epoxy which shows moderately high transmittance (50%-70%) and Anycubic Standard Clear Resin showing the lowest of them all between 40%-60%.

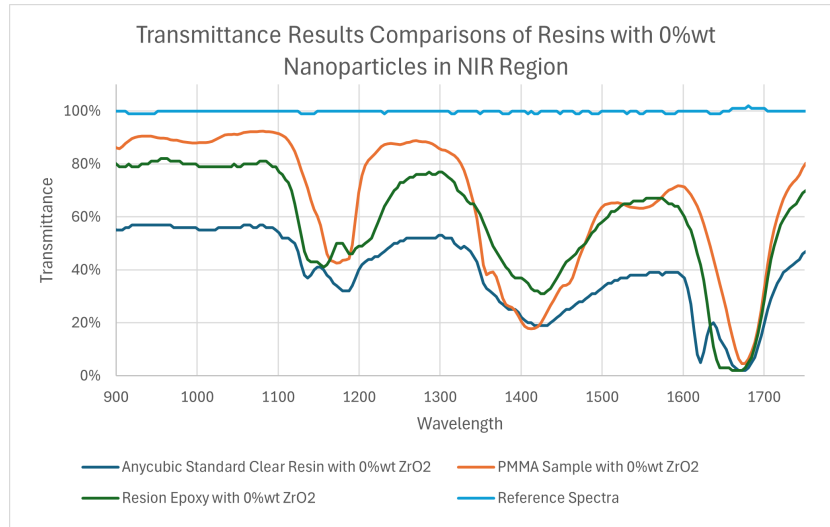


**Figure 6.2:** Transmittance Comparison in NIR Region of Resins without Nanoparticles

### 6.1.2 Transmittance Comparison of Resins with Nanoparticles

A similar trend is seen even in the case of samples with nanoparticles where the PMMA sample reaches the highest transmittance value at a shorter wavelength, followed by the Resion epoxy and Anycubic Standard Clear Resin. Amongst all the samples where the Resion epoxy and PMMA sample reach similar transmittance values around 800nm wavelength, the Anycubic sample exhibits a much lower transmittance.

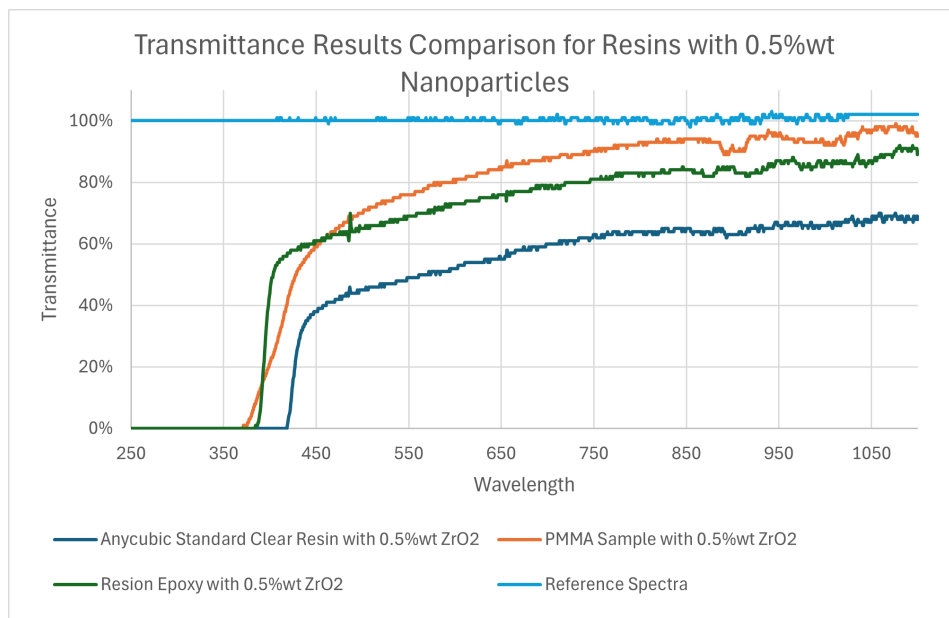


**Figure 6.3:** Transmittance Comparison of Resins with Nanoparticles

The transmittance for PMMA sample with nanoparticles remains fairly similar to the transmittance in the sample without nanoparticles (around 80%). However, the transmittance for Resion epoxy and the Anycubic



resin reduces significantly with having similar dips at 1200nm, 1400nm and 1600nm wavelengths.

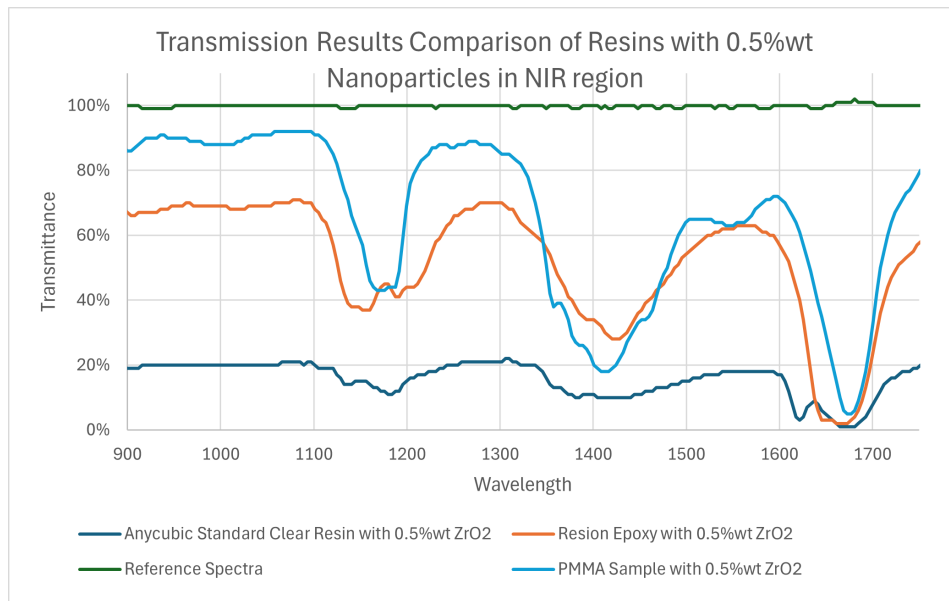


**Figure 6.4:** Transmittance Comparison in NIR Region of Resins with Nanoparticles

### 6.1.3 Transmittance Comparison of Commercial UV Curable Resins

Amongst the commercial UV curable resins, the Elegoo Standard Photopolymer Resin shows the highest transmittance (95%), SIRAYA Tech Professional UV Curable Resin showing the lowest around 60-70% and other resins varying between 80-90%.

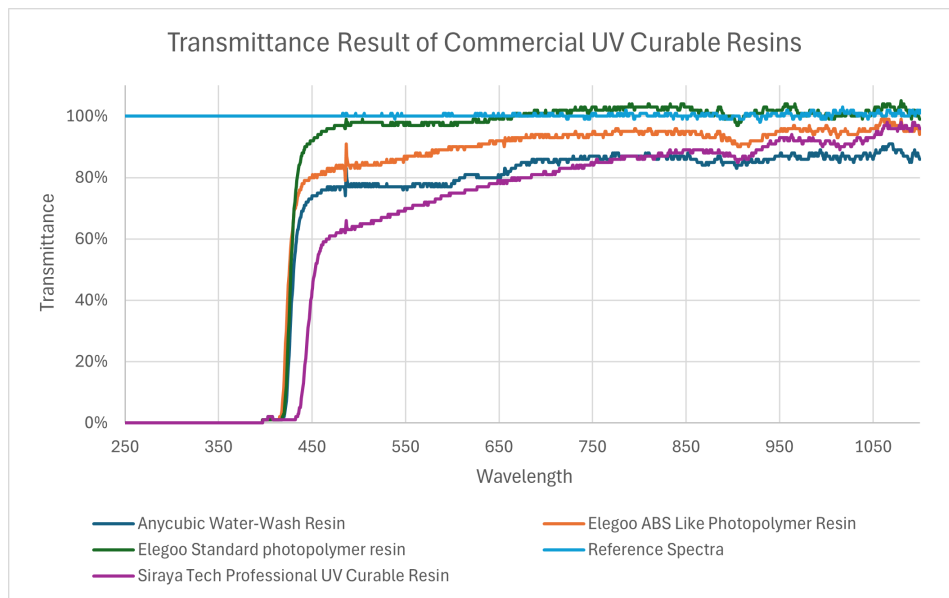


**Figure 6.5:** Transmittance of Commercial UV Curable Resins

Similar trend is also observed for resins in NIR region, where Elegoo Standard Photopolymer Resin shows a transmittance between 80-90% and SIRAYA Tech Professional UV Curable Resin showing the lowest transmittance around 50-60%.

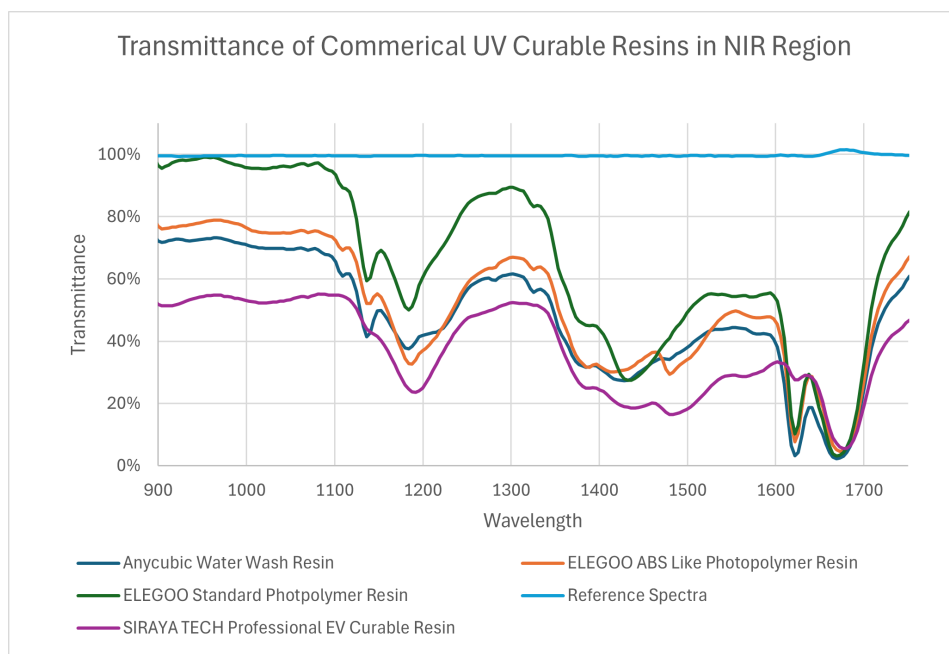


**Figure 6.6:** Transmittance of Commercial UV Curable Resins in NIR Region

#### 6.1.4 Transmittance Results Comparison for Commercial Resins with Various Concentrations of Nanoparticles

Additional samples are prepared with Anycubic Standard Clear Resin and Elegoo Standard Photopolymer Resin with varying concentrations of nanoparticles added to see if the trend of transmittance decreasing by adding nanoparticles is followed.

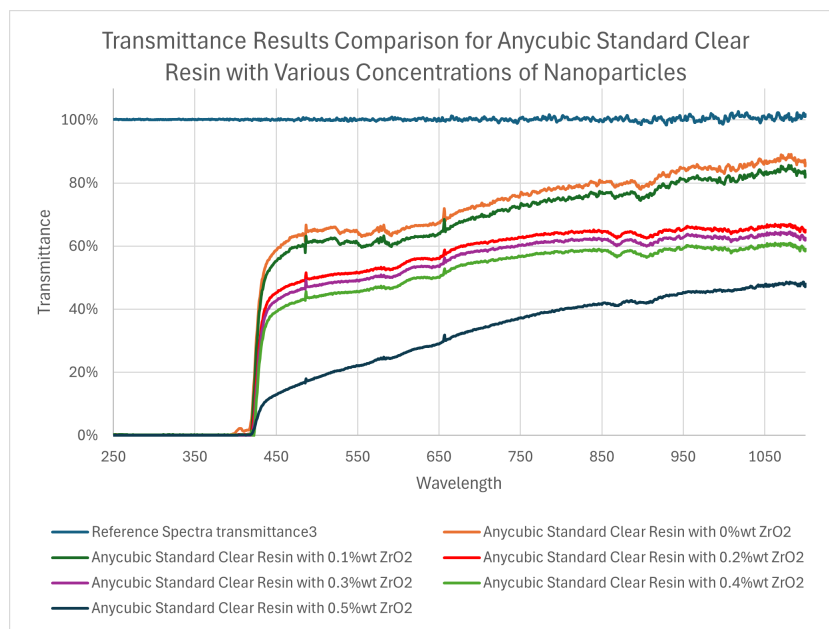


**Figure 6.7:** Transmittance Results Comparison for Anycubic Standard Clear Resin with varying Concentration of Nanoparticles

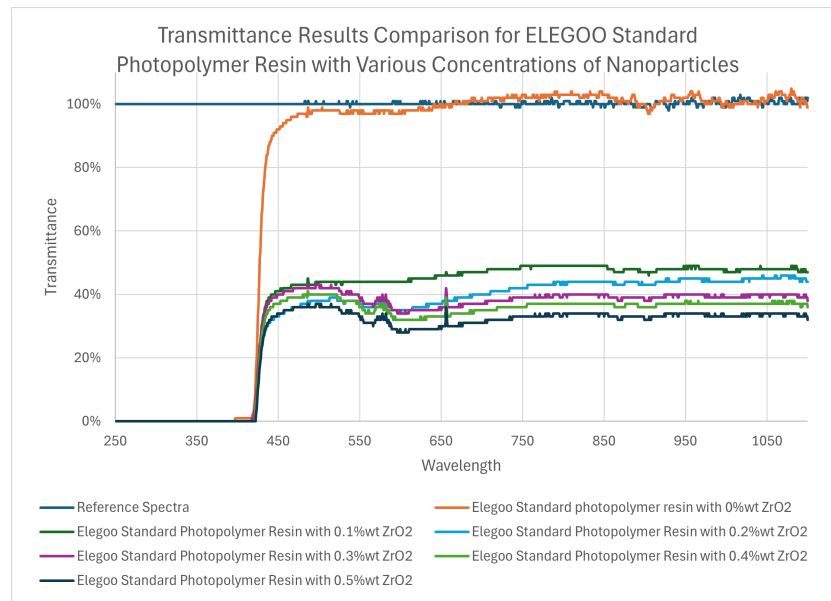


**Figure 6.8:** Transmittance Results Comparison for Elegoo Standard Photopolymer Resin with varying Concentration of Nanoparticles

## Chapter 7

# Conclusion and Future Work

Various significant insights were gained during my research. After conducting optical characteristics tests on the prepared UV- resin samples embedded with nanoparticles, several key findings emerge. This chapter will talk in detail about those findings, their implications, and the aspects that can be looked into for future research.

### 7.0.1 Dispersion of $\text{ZrO}_2$ Nanoparticles

The nanoparticles are water-based solutions, but epoxy is hydrophobic. Another factor to consider is that PMMA can be dissolved in acetone. A combination of the  $\text{ZrO}_2$  solution and the PMMA solution led to a cloudy and inhomogeneous solution while the sediments settled at the bottom. This problem is tackled by evaporating the water from  $\text{ZrO}_2$  nanoparticle solution and then re-dispersion in acetone. Thus, a proper and uniform mixing of nanoparticles in all samples is possible.

### 7.0.2 Performance Comparison of DMPA Photoinitiator

The performance of photoinitiator DMPA with PMMA is excellent. However, it shows poor interactions with epoxy. The cross-linking for epoxy resins to be more effective is cationic polymerization, whereas DMPA functions by a free radical polymerization mechanism. This incompatibility resulted in yellowing in the epoxy sample after UV curing.

### 7.0.3 Curing Speed Comparison

The curing times for the different samples show a stark difference. The epoxy sample takes around 3 hours to cure completely. The PMMA sample, on the other hand, takes approximately 1.5 hours to heal fully. Meanwhile, the already properly photoinitiated mixture of Anycubic Standard clear resin available in the market is cured within only 1 minute of DMPA addition. In the case of the PMMA sample, shrinkage in the UV-cured sample is observed over 12-18 hours, where the part of the sample in contact with the cuvette walls shrinks and forms a white layer around the walls as seen in Figure 5.1 , affecting the transmittance of the sample.

## 7.1 Optical Properties Analysis of Prepared Resin Samples

As seen from the results in Figure 6.1, the PMMA sample shows the highest transmittance value of between 85-95% from a lower value of wavelength (450nm) in the UV and visible light region and between 80-90% in the NIR region. This shows that adding a DMPA photoinitiator optimizes the cross-linking much better in an epoxy. Even though the Anycubic Standard Clear Resin is a mixture of epoxy and acrylate, it also should have similar transmittance. The still existence of hydroxy cyclohexyl phenyl ketone as a photoinitiator is what makes the difference.

The addition of nanoparticles decreases the transmittance in the case of all the resins. Zirconium dioxide ( $\text{ZrO}_2$ ), having a particle diameter of 100nm like the ones used in this research, absorbs light mainly in the UV region ( $\leq 300\text{nm}$ ) corresponding to the transition from the valence band to the conduction band. The wide bandgap of  $\text{ZrO}_2$  (around 5–7 eV) ensures their strong absorption is in the UV range, so they are effective for UV-blocking applications without affecting visible light transmission [59].

## 7.2 Future Scope for Research

Future research can thus focus on the usage of a cationic photoinitiator like Diphenyl 4-(phenylthio) phenylsulfonium Hexafluoroantimonate in a bid to improve cure efficiency and for better compatibility with epoxy resins as an attempt to overcome the limitations faced by DMPA [60]. Further characterization, for example, ellipsometry or refractometry, can be applied to perform detailed measurements of the refractive index in the resins cured by UV and provide deeper insight into the cross-linking density, uniformity, and overall optical quality. The optimization of alternative photoinitiators in conjunction with detailed optical characterization can result in the development of an optimized formulation and processing technique for high-performance UV-cured epoxy resins.

Currently, while configuring modifications on the printer, the custom PCB and Raspberry Pi is designed to control the projector and DMD device which gives us control over the exposure settings of the printer. However, in order to successfully conduct multi-material DLP printing, control over the z-stage by programming the stepper motor is also required.

# Bibliography

- [1] Brian McCall, Tomasz S Tkaczyk, R S Weinstein, M R Descour, C Liang, G Barker, K M Scott, L Richter, E A Krupinski, A K Bhattacharyya, J R Davis, A R Graham, M Rennels, W C Russum, J F Goodall, P Zhou, A G Olszak, B H Williams, J C Wyant, and P H Bartels. 0220) optical design and fabrication; (220.1920) diamond machining; (220.3630) lenses; (220.4610) optical fabrication, 2013.
- [2] Andrew M. Boyd. Optical design of athermal, multispectral, radial gradient-index lenses. *Optical Engineering*, 57:1, 8 2018.
- [3] Andrew M. Boyd. Optical design of multi-material, general rotationally symmetric grin lenses. In *Proceedings of SPIE-Intl Soc Optical Eng*, volume 2019, page 19, 5 2019.
- [4] Hao Lv, Aimei Liu, Jufang Tong, Xunong Yi, and Qianguang Li. Gradient refractive index square lenses. i. fabrication and refractive index distribution, 2009.
- [5] Gregory Berglund, Anna Wisniowiecki, John Gawedzinski, Brian Applegate, and Tomasz S. Tkaczyk. Additive manufacturing for the development of optical/photonic systems and components. *Optica*, 9:623, 6 2022.
- [6] Nagendra Nag, Santosh Jha, Suri Sastri, Lee M. Goldman, Peter McCarthy, Greg R. Schmidt, Julie L. Bentley, and Duncan T. Moore. Alon grin optics for visible-mwir applications. In *Advanced Optics for Defense Applications: UV through LWIR*, volume 9822, page 98220V. SPIE, 5 2016.
- [7] Changliang Guo, Tara Urner, and Shu Jia. 3d light-field endoscopic imaging using a grin lens array. *Applied Physics Letters*, 116, 3 2020.
- [8] Manuel Rank and Andreas Heinrich. Measurement and use of the refractive index distribution in optical elements created by additive manufacturing. In *Proceedings of SPIE-Intl Soc Optical Eng*, page 35, 10 2020.
- [9] Weisong Wang. Development of a polymer-based gradient refractive index structure and actuation mechanisms for optical lens applications, 2004.
- [10] Yizhen Zhu, Tengting Tang, Suyi Zhao, Dylan Joralmon, Zachary Poit, Bhushan Ahire, Sanjay Keshav, Aaditya Rajendra Raje, Joshua Blair, Zilong Zhang, and Xiangjia Li. Recent advancements and applications in 3d printing of functional optics, 4 2022.
- [11] Florian Bociort. Imaging properties of gradient-index lenses.
- [12] C. Gomez-Reino and M. I. Perez. Gradient-index optics: Fundamentals and applications. *Gradient-Index Optics: Fundamentals and Applications*, 2002.
- [13] Hossein Salmani Rezaei, Gerrit Hohenhoff, Peter Jäschke, Stefan Kaierle, and Ludger Overmeyer. Design and fabrication of multilayer grin lenses by multi-material additive manufacturing for light coupling applications in planar optoelectronic systems. In *Proceedings of SPIE-Intl Soc Optical Eng*, page 54, 2 2020.
- [14] Chen Wang, Venkateshwar Madka, Feng Yan, Sanjay G. Patel, Chinthalapally V. Rao, and Qinggong Tang. Laparoscopic optical coherence tomography system for 3d bladder tumor detection. In *SPIE-Intl Soc Optical Eng*, page 17, 3 2021.

- [15] Andrea Sattin, Andrea Antonini, Serena Bovetti, Claudio Moretti, Angelo Forli, Francesca Succol, Vijayakumar P. Rajamanickam, Andrea Bertoncini, Carlo Liberale, and Tommaso Fellin. Extended field-of-view microendoscopy through aberration corrected grin lenses. In *Optics InfoBase Conference Papers*, 2019.
- [16] Rishabh Magazine, Bas van Bochove, Sedigheh Borandeh, and Jukka Seppälä. 3d inkjet-printing of photo-crosslinkable resins for microlens fabrication. *Additive Manufacturing*, 50, 2 2022.
- [17] Kenji Takada, Hong Bo Sun, and Satoshi Kawata. Improved spatial resolution and surface roughness in photopolymerization- based laser nanowriting. *Applied Physics Letters*, 86:1–3, 2 2005.
- [18] N. Tadokoro, K. Jaisupap, A. Sukbumperng, S. Pannakarn, S. Khraikratoke, P. Jamnongpian, and N. Iwata. Investigation of shrinkage and cracking of ophthalmic lens coating by a cycle test of uv radiation and high humidity. In *Thin Solid Films*, volume 520, pages 4169–4173, 4 2012.
- [19] Emma Geisler, Maxime Lecomperre, and Olivier Soppera. 3d printing of optical materials by processes based on photopolymerization: materials, technologies, and recent advances. *Photonics Research*, 10:1344, 6 2022.
- [20] Monika Topa-Skwarczyńska and Joanna Ortyl. Photopolymerization shrinkage: strategies for reduction, measurement methods and future insights. *Polymer Chemistry*, 14:2145–2158, 4 2023.
- [21] K. Wang and Z. Z. Wang. An improved method for accurate measurement of material shrinkage during photopolymerization. *Experimental Mechanics*, 63:125–138, 1 2023.
- [22] Christian R. Ocier, Corey A. Richards, Daniel A. Bacon-Brown, Qing Ding, Raman Kumar, Tanner J. Garcia, Jorik van de Groep, Jung Hwan Song, Austin J. Cyphersmith, Andrew Rhode, Andrea N. Perry, Alexander J. Littlefield, Jinlong Zhu, Dajie Xie, Haibo Gao, Jonah F. Messinger, Mark L. Brongersma, Kimani C. Toussaint, Lynford L. Goddard, and Paul V. Braun. Direct laser writing of volumetric gradient index lenses and waveguides. *Light: Science and Applications*, 9, 12 2020.
- [23] James A. Corsetti, Greg R. Schmidt, and Duncan T. Moore. Design and characterization of a copolymer radial gradient index zoom lens. In *Novel Optical Systems Design and Optimization XVII*, volume 9193, page 91930U. SPIE, 9 2014.
- [24] Taiki Maruyama, Hotaka Hirata, Taichi Furukawa, and Shoji Maruo. Multi-material microstereolithography using a palette with multicolor photocurable resins. *Optical Materials Express*, 10:2522, 10 2020.
- [25] Xiangfan Chen, Wenzhong Liu, Biqin Dong, Jongwoo Lee, Henry Oliver T. Ware, Hao F. Zhang, and Cheng Sun. High-speed 3d printing of millimeter-size customized aspheric imaging lenses with sub 7 nm surface roughness. *Advanced Materials*, 30, 5 2018.
- [26] John R. Tumbleston, David Shirvanyants, Nikita Ermoshkin, Rima Januszewicz, Ashley R. Johnson, David Kelly, Kai Chen, Robert Pinschmidt, Jason P. Rolland, Alexander Ermoshkin, Edward T. Samulski, and Joseph M. DeSimone. Continuous liquid interface production of 3d objects. *Science*, 347:1349–1352, 3 2015.
- [27] Martin P De Beer, Harry L Van Der Laan, Megan A Cole, Riley J Whelan, Mark A Burns, and Timothy F Scott. Rapid, continuous additive manufacturing by volumetric polymerization inhibition patterning, 2019.
- [28] Alessandra Vitale, Matthew G. Hennessy, Omar K. Matar, and João T. Cabral. Interfacial profile and propagation of frontal photopolymerization waves. *Macromolecules*, 48:198–205, 1 2015.
- [29] E. Persempé, C. Parra-Cabrera, C. Clasen, and R. Ameloot. Binder-jetting 3d printer capable of voxel-based control over deposited ink volume, adaptive layer thickness, and selective multi-pass printing. *Review of Scientific Instruments*, 92, 12 2021.
- [30] Xavier Porte, Niyazi Ulas Dinc, Johnny Moughames, Giulia Panusa, Caroline Juliano, Muamer Kadic, Christophe Moser, Daniel Brunner, and Demetri Psaltis. Direct (3+1)d laser writing of graded-index optical elements. *Optica*, 8:1281, 10 2021.

- [31] Usman Shaukat, Elisabeth Rossegger, and Sandra Schlögl. A review of multi-material 3d printing of functional materials via vat photopolymerization, 6 2022.
- [32] Kathleen L. Sampson, Bhavana Deore, Abigail Go, Milind Ajith Nayak, Antony Orth, Mary Gallerneault, Patrick R.L. Malenfant, and Chantal Paquet. Multimaterial vat polymerization additive manufacturing, 9 2021.
- [33] Kehui Hu, Pengcheng Zhao, Jianjun Li, and Zhigang Lu. High-resolution multiceramic additive manufacturing based on digital light processing. *Additive Manufacturing*, 54, 6 2022.
- [34] Elisabeth Rossegger, Jakob Strasser, Rita Höller, Mathias Fleisch, Michael Berer, and Sandra Schlögl. Wavelength selective multi-material 3d printing of soft active devices using orthogonal photoreactions. *Macromolecular Rapid Communications*, 44(2):2200586, 2022.
- [35] Chi Zhou, Yong Chen, Zhigang Yang, and Behrokh Khoshnevis. Digital material fabrication using mask-image-projection-based stereolithography. *Rapid Prototyping Journal*, 19:153–165, 2013.
- [36] Nano3DTech. Nano3dtech - 3d printing materials and solutions. Available at: <https://www.nano3dtech.com/>. Accessed: 2024-08-09.
- [37] openMLA contributors. Elegoo mars 4 dlp controller. <https://github.com/openMLA/elegoo-mars-4-dlp-controller>, 2024.
- [38] Schematic for raspberry pi dmd controller board. Available at: [https://drive.google.com/drive/folders/1\\_Az6TJDA8nMaeGoxmn9SUhRAFrNds27?usp=sharing](https://drive.google.com/drive/folders/1_Az6TJDA8nMaeGoxmn9SUhRAFrNds27?usp=sharing), 2024. Accessed: 2024-08-09.
- [39] Laura L Beecroft and Christopher K Ober. Reviews nanocomposite materials for optical applications, 1997.
- [40] Qingyan Zhang, Chi Huang, Hongxia Wang, Mingjie Hu, Houbin Li, and Xinghai Liu. Uv-curable coating crosslinked by a novel hyperbranched polyurethane acrylate with excellent mechanical properties and hardness. *RSC Advances*, 6:107942–107950, 2016.
- [41] Mohammad Syuhaimi Ab. Rahman, Khaled Mohamed Shaktur, Rahmah Mohammad, Wan Aimi Zalikha, Norwimie Nawi, and Ahmad Faiza Mohd. Optical properties and indentation hardness of thin-film acrylated epoxidized oil. *Optical Engineering*, 51(2):025002–025002–9, 2012.
- [42] Cristian Mendes-Felipe, Juliana Oliveira, Ikerne Etxebarria, José Luis Vilas-Vilela, and Senentxu Lanceros-Mendez. State-of-the-art and future challenges of uv curable polymer-based smart materials for printing technologies, 3 2019.
- [43] Jung Dae Cho and Jin Who Hong. Uv-initiated free radical and cationic photopolymerizations of acrylate/epoxide and acrylate/vinyl ether hybrid systems with and without photosensitizer. *Journal of Applied Polymer Science*, 93:1473–1483, 8 2004.
- [44] Mostafa Mabrouk, Gehan T. El-Bassyouni, Hanan H. Beherei, Sayed H. Kenawy, and Esmat M.A. Hamzawy. Inorganic additives to augment the mechanical properties of 3D-printed systems. *Advanced 3D-Printed Systems and Nanosystems for Drug Delivery and Tissue Engineering*, 2020.
- [45] Uwe Gleissner and Thomas Hanemann. Tailoring the optical and rheological properties of an epoxy acrylate based host-guest system. *Optical Engineering*, 53(8):087106, 2014.
- [46] Guoyan Zhang, Mei Chen, Jibin Zhang, Baofeng He, Huai Yang, and Bai Yang. Effective increase in the refractive index of novel transparent silicone hybrid films by introduction of functionalized silicon nanoparticles. *RSC Advances*, 5:62128–62133, 2015.
- [47] C. Decker and K. Moussa. Kinetic study of the cationic photopolymerization of epoxy monomers. *Journal of Polymer Science Part A: Polymer Chemistry*, 28:3429–3443, 1990.
- [48] Aleksandr Ovsianikov, Jacques Viertl, Boris Chichkov, Mohamed Oubaha, Brian MacCraith, Ioanna Sakellari, Anastasia Giakoumaki, David Gray, Maria Vamvakaki, Maria Farsari, and Costas Fotakis. Ultra-low shrinkage hybrid photosensitive material for two-photon polymerization microfabrication. *ACS Nano*, 2:2257–2262, 11 2008.



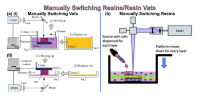
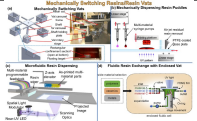
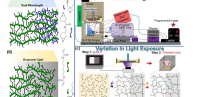
- [49] V. Shukla, M. Bajpai, D. K. Singh, M. Singh, and R. Shukla. Review of basic chemistry of uv-curing technology, 10 2004.
- [50] M.D. Healy, P.C. Guschl, X. Wang, and M.A. Weinstein. Inkjet printing of high index zirconia nanocomposite materials. *TechConnect Briefs*, pages 137–140, 2017.
- [51] Material safety data sheet: Abs like photopolymer resin. Available at: [https://drive.google.com/drive/folders/1\\_Az6TJDA8nMaeGoxmn9SUhRAFrtnDs27?usp=drive\\_link](https://drive.google.com/drive/folders/1_Az6TJDA8nMaeGoxmn9SUhRAFrtnDs27?usp=drive_link), 2020. Accessed: 2024-08-09.
- [52] Material safety data sheet: Standard photopolymer resin. Available at: [https://drive.google.com/drive/folders/1\\_Az6TJDA8nMaeGoxmn9SUhRAFrtnDs27?usp=drive\\_link](https://drive.google.com/drive/folders/1_Az6TJDA8nMaeGoxmn9SUhRAFrtnDs27?usp=drive_link), 2022. Accessed: 2024-08-09.
- [53] Material safety data sheet: Standard colored resin. Available at: [https://drive.google.com/drive/folders/1\\_Az6TJDA8nMaeGoxmn9SUhRAFrtnDs27?usp=drive\\_link](https://drive.google.com/drive/folders/1_Az6TJDA8nMaeGoxmn9SUhRAFrtnDs27?usp=drive_link), 2020. Accessed: 2024-08-09.
- [54] Material safety data sheet: Water-wash resin clear. Available at: [https://drive.google.com/drive/folders/1\\_Az6TJDA8nMaeGoxmn9SUhRAFrtnDs27?usp=drive\\_link](https://drive.google.com/drive/folders/1_Az6TJDA8nMaeGoxmn9SUhRAFrtnDs27?usp=drive_link), 2020. Accessed: 2024-08-09.
- [55] J. N. Hilfiker. *In situ spectroscopic ellipsometry (SE) for characterization of thin film growth*, pages 99–132. William Andrew, 2011.
- [56] Shikhar Mohan, Eiji Kato, James K. III Drennen, and Carl A. Anderson. Refractive Index Measurement of Pharmaceutical Solids: A Review of Measurement Methods and Pharmaceutical Applications. *Journal of Pharmaceutical Sciences*, 108(9):3478–3495, July 2019.
- [57] Ming-Horng Chiu, Ju-Yi Lee, and Der-Chin Su. Refractive-index measurement based on the effects of total internal reflection and the uses of heterodyne interferometry. *Applied Optics*, 36(13):2936–2939, 1997.
- [58] Jesper Jung, Jakob Bork, Tobias Holmgaard, and Niels Anker Kortbek. Ellipsometry. Project report, Aalborg University, Institute of Physics and Nanotechnology, Aalborg Øst, Denmark, December 2004. Detection of Nanostructures, Project Group 116.
- [59] N. C. Horti, M. D. Kamatagi, S. K. Nataraj, M. S. Sannaikar, and S. R. Inamdar. Photoluminescence properties of zirconium oxide (zro2) nanoparticles. *AIP Conference Proceedings*, 2274:020002, 2020.
- [60] Mazhar Peerzada, Sadaf Abbasi, Kin Tak Lau, and Nishar Hameed. Additive Manufacturing of Epoxy Resins: Materials, Methods, and Latest Trends. *Industrial & Engineering Chemistry Research*, 59(14):6375–6390, 2020.

# Appendix A

## Appendix

Extra information

**Table A.1:** Various Categories of Multi-Material Vat Photopolymerization Techniques

Method	Description	Image
Manual switching of Resins/Resin Vats	To add different materials to a 3D printed object using vat polymerization, pause the print and manually switch the resins or vats. The resin vat and printed part may be washed and dried manually to avoid contamination.	 A schematic diagram showing a resin vat being manually switched. It includes a reservoir, a pump, and a nozzle. The process involves pausing the print, switching the resin, and then continuing the print. The diagram is labeled 'Manually Switching Resins/Resin Vats'.
Mechanical Switching of Resins/Resin Vats	Customizations includes mechanical components that can remove one material, clean the resin vat and partially printed part, and add new material.	 A schematic diagram showing a mechanical switching system. It includes a reservoir, a pump, and a nozzle. The process involves pausing the print, switching the resin, and then continuing the print. The diagram is labeled 'Mechanically Switching Resins/Resin Vats'.
Dual Wavelength Curing and Variation in Light exposure	VAT polymerization allow for the creation of multi-material objects by selectively initiating radical and cationic polymerizations in desired locations using two different wavelength light sources. Controlling polymerization can create defined regions with different mechanical properties within a 3D object. Light intensity and exposure time impact cross-linking density, resulting in elastic modulus and response to stimuli. Lower light doses have created sacrificial support structures that can be easily removed during postprocessing.	 A schematic diagram showing a dual wavelength curing system. It includes a reservoir, a pump, and a nozzle. The process involves pausing the print, switching the resin, and then continuing the print. The diagram is labeled 'Dual Wavelength'.

**Table A.2:** Benefits and Drawbacks of Each Technique

Methods	Benefits	Limitations
Manual Switching Resins/Resin Vats	<ul style="list-style-type: none"> <li>• Simplest method</li> <li>• Noncomplex formulation of multiple separate resins</li> <li>• Large number of possible resin formulations</li> </ul>	<ul style="list-style-type: none"> <li>• Slow</li> <li>• Extra washing/drying steps to avoid potential contamination</li> <li>• Possible issues with interfacial adhesion</li> <li>• Previously built layers can block light preventing proper curing of subsequent layers</li> <li>• Difficult to print entrapped materials</li> <li>• Irregular surfaces between materials and uneven or poorly adhered final parts due to surface tension between resin and cured polymer</li> <li>• Possible differences in dimensions between materials</li> <li>• Requires extra programming to enable stopping printing and starting at various heights</li> </ul>
Mechanically Switching Resins/Resin Vats	<ul style="list-style-type: none"> <li>• Noncomplex formulation of multiple separate resins</li> <li>• Large number of possible resin formulations</li> </ul>	<ul style="list-style-type: none"> <li>• Extra washing/drying steps to avoid potential contamination</li> <li>• Possible issues with interfacial adhesion</li> <li>• Previously built layers can block light preventing proper curing of subsequent layers</li> <li>• Difficult to print entrapped materials</li> <li>• Irregular surfaces between materials and uneven or poorly adhered final parts due to surface tension between resin and cured polymer</li> <li>• Possible differences in dimensions between materials</li> <li>• Custom software or programming to enable stopping printing and switching resins</li> </ul>
Dual Wavelength	<ul style="list-style-type: none"> <li>• A single resin formulation with orthogonal chemistry mechanisms</li> </ul>	<ul style="list-style-type: none"> <li>• Additional hardware and software for integrating more than one wavelength light source</li> <li>• Orthogonal chemistry precursors must be miscible</li> </ul>
Variation in Light Parameters	<ul style="list-style-type: none"> <li>• A single resin formulation</li> </ul>	<ul style="list-style-type: none"> <li>• Software to incorporate differences in light exposure time, intensity by location</li> <li>• Possible adjustments in printing area due to dimensional differences between degree of cure</li> </ul>

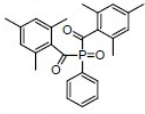
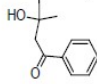
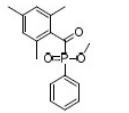
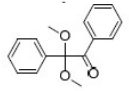
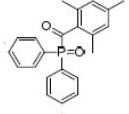
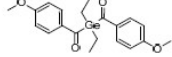
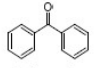
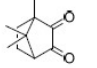
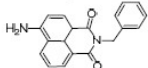
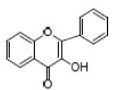
Photoinitiators	Absorption Wavelength	Structure
Phenyl bis (2,4,6-trimethylbenzoyl) phosphine oxide (BAPO)	295 nm, 370 nm	
2-Hydroxy-2-methyl-1-phenyl-propan-1-one (Irgacure 1173)	245 nm, 280 nm, 331 nm	
Ethyl (2,4,6-trimethylbenzoyl) phosphine oxide (Irgacure TPO-L)	275 nm, 379 nm	
2,2-dimethoxy-1-phenylacetophenone (Irgacure 651)	252 nm, 340 nm	
Diphenyl (2,4,6-trimethylbenzoyl) phosphine oxide (Irgacure TPO)	295 nm, 368 nm, 380 nm, 393 nm	
Bis (4-methoxybenzoyl) diethylgermanium (Ivocerin)	408 nm	
Benzophenone	253 nm	
Camphorquinone	468 nm	
5-amino-2-benzyl-1H-benzisoquinoline-1,3(2H)-dione (NDP2)	417 nm	
3-hydroxyflavone (3HF)	370–470 nm	

Figure A.1: List of radical photoinitiators used in vat photopolymerization 3D printing

## A.1 Materials Buy List

The table below shows the buy list for the materials that are ordered for preparing the ink samples.

Materials	Manufacturer	Quantity	Price
RESION UV Epoxy resin	PolyesterShoppen	800g	€ 25,99
Zirconium (IV) Oxide (CAS No: 1314-23-4)	Sigma Aldrich	100ml	€ 173,00
DMPA Photoinitiator (CAS RN: 24650-42-8)	TCI Chemicals	25g	€ 34,00
Anycubic, 3D printing UV Sensitive Resin(Clear)	Anycubic	1kg	€ 18,14
Polymethyl Methacrylate (PMMA)	TCI Chemicals	500g	€ 71,00

Table A.3: Materials Buy List

A.2 Specifications of Elegoo Mars 4 DLP Printer

Specification	Details
Build Volume	132.8 x 74.7 x 150 mm <sup>3</sup>
Light Source	TI optical machine + full grayscale anti-aliasing algorithm, LED light source
Operating Screen	3.5-inch resistive touch screen
Heat Dissipation Method	Fanless design, printing noise below 48db
Printing Speed	30-70 mm/h
LCD Screen Size	No
Language	Chinese, English
Dimensions	246 x 230 x 453 mm <sup>3</sup>
Layer Thickness	0.01-0.2 mm
LCD Screen Protector	Ultra clear tempered glass
Air Purifier	Plug-in
Net Weight	6.8 kg
XY Resolution	0.05 mm (2560*1440)
Connection Method	USB offline printing
Other Functions	N.A.
Gross Weight	10.34 kg
Z-Axis Accuracy	0.02 mm
System	EL3D-3.0.2
Resin	Supports most resins on the market (water-washable, standard, ABS-like, plant-based, etc.)
Printing Technology	DLP
Slicing Software	Voxeldance Tango
Power Requirements	100-240V 50/60Hz 12V 1.5A 18W

Table A.4: Specifications of the Elegoo Mars 4 DLP Printer

A.2.1 Electronic Configuration of the Printer

The DLPC1438 3D print controller is designed to manage the operation of DLP300S and DLP301S digital micromirror devices used in the Elegoo Mars 4 DLP printer. This digital controller facilitates a convenient interface between the electronics and the DMD.

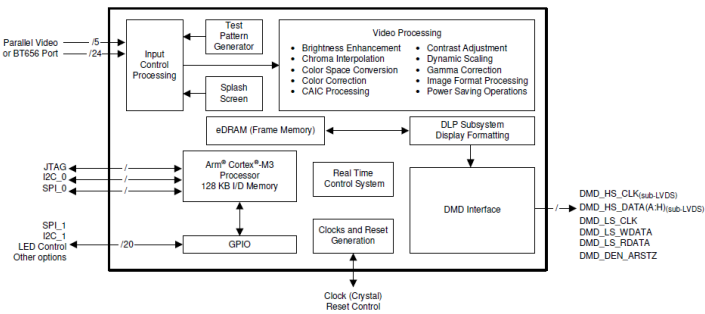
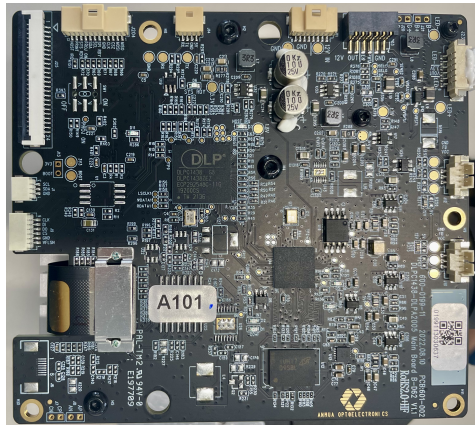


Figure A.2: Functional Block Diagram for DLPC 1438 Controller



**Figure A.3:** DLPC 1438 Controller Board

Some of the key features of the digital controller, as described below, prove it's efficient for a DLP printer.

- **DLP Technology:** Optimized for DLP300S and DLP301S (0.3-inch 3.6-megapixel) DMDs.
- **3D Printing Specifics:**
  - Supports linear gamma modes for improved illumination uniformity and grayscale printing.
  - Programmable layer exposure time.
  - 8-bit monochrome grayscale output.
- **System Integration:**
  - Front-end FPGA with SPI data input interface.
  - Actuator control for precise movement.
  - I2C control for device configuration.
  - Programmable LED current control for consistent light output.
- **Reliability:** Designed for stable operation in DLP 3D printer environments.
- **Power Management:** Works with DLPA2000, DLPA2005, DLPA3000, or DLPA3005 PMICs and LED drivers for efficient power handling.

Understanding the architecture of the DLPC 1438 controller board is necessary to help us get deeper insights into the parameters that can be controlled when we gain access to some of its ports.

- **Microcontroller Unit (MCU):**
  - Executes firmware for data processing and control tasks.
  - Manages decompression of video data, synchronization, and power management.
- **Memory Interface:**
  - Interfaces with external memory (e.g., DRAM or Flash) for storing image data and firmware.
  - Ensures fast data access and transfer rates.
- **Digital Signal Processing (DSP):**
  - Handles complex calculations for image scaling, color correction, and other video processing tasks.
  - Ensures high-quality prints.
- **Input/Output (I/O) Interfaces:**
  - Multiple I/O interfaces including HDMI, MIPI, and parallel data interfaces for receiving image data.
  - Control interfaces like I2C and SPI for communication with other system components.
- **Power Management Unit (PMU):**

- Ensures efficient power distribution to all parts of the controller and the DMD.
- Manages different power modes to optimize energy consumption.
- **Control Logic:**
  - Coordinates timing and operations across the DMD, light source, and other peripherals.
  - Ensures accurate mirror tilting in the DMD for precise light modulation and image formation.
- **Programmable Features:**
  - Supports programmable layer exposure times.
  - Programmable LED current control for consistent and reliable 3D printing.

To power the printer along with its components like the projector, stepper motor, and other peripherals that can be connected, a power supply unit also plays an important role where the output pins like the i2c pins from the projector controller board, the pins from the stepper motor and an external air purifier that can be installed need to be powered from the same board for smooth functioning of the printer. The LCD from where the printer can be operated is also connected to this board.

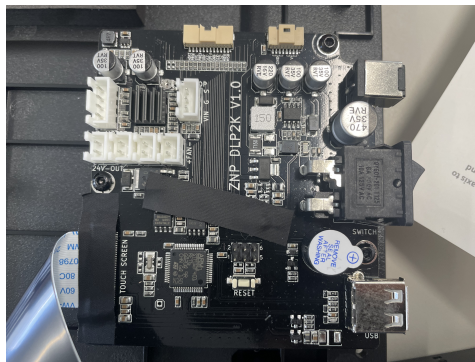


**Figure A.4:** Power Supply Unit

A.3 Individual Transmittance Results for Resins without Nanoparticles

Individual Transmittance Results for Resins without Nanoparticles

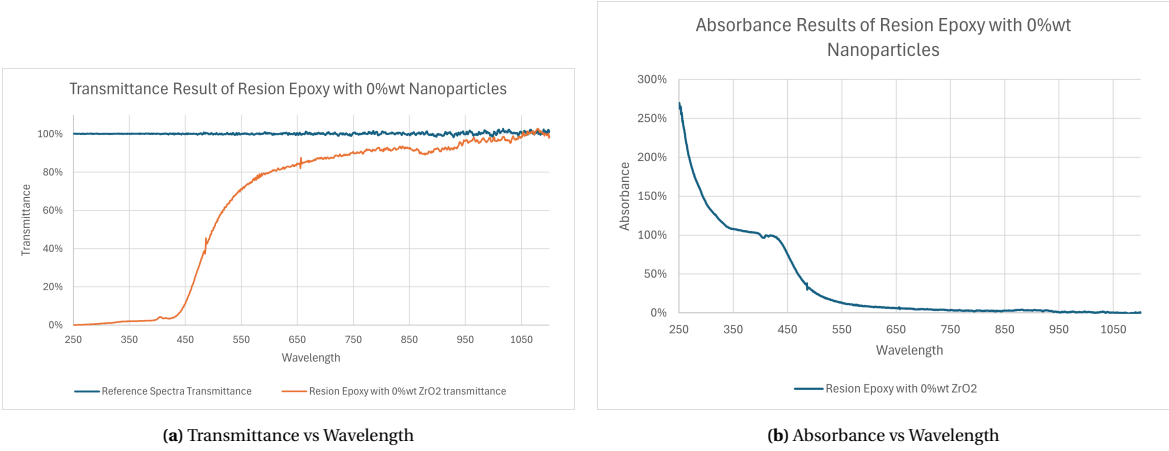


Figure A.5: Spectroscopy Test Results for Resion Epoxy Sample

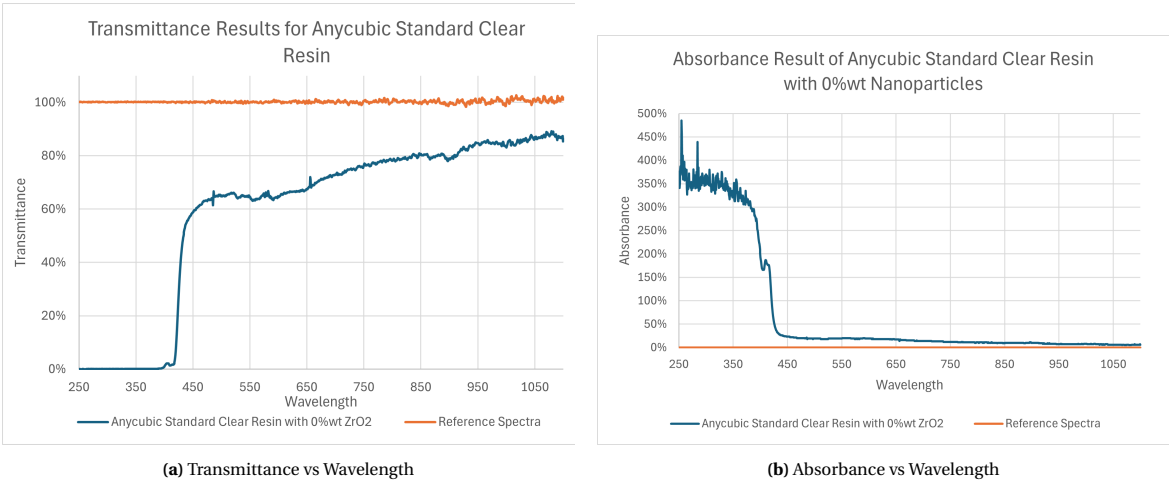


Figure A.6: Spectroscopy Test Results for Anycubic Standard Clear Resin Sample

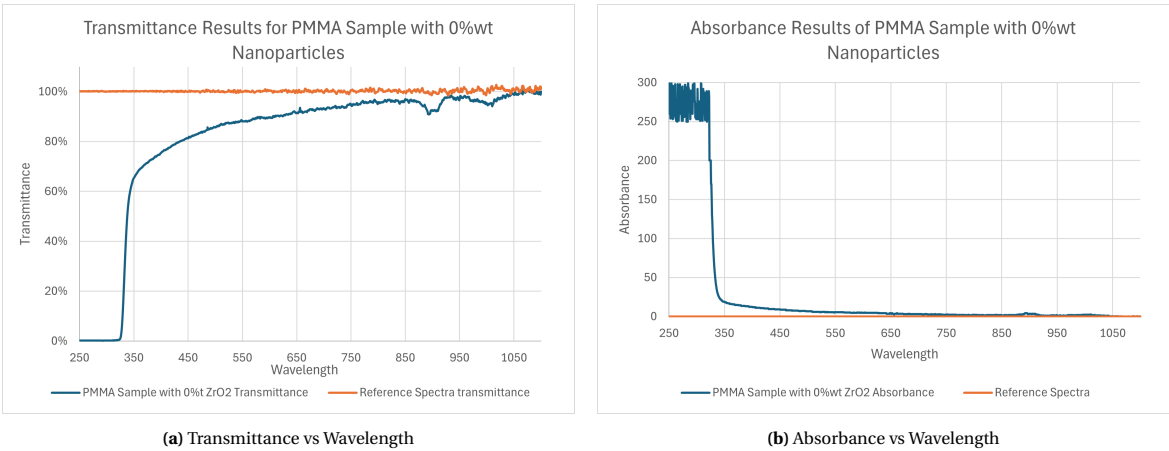
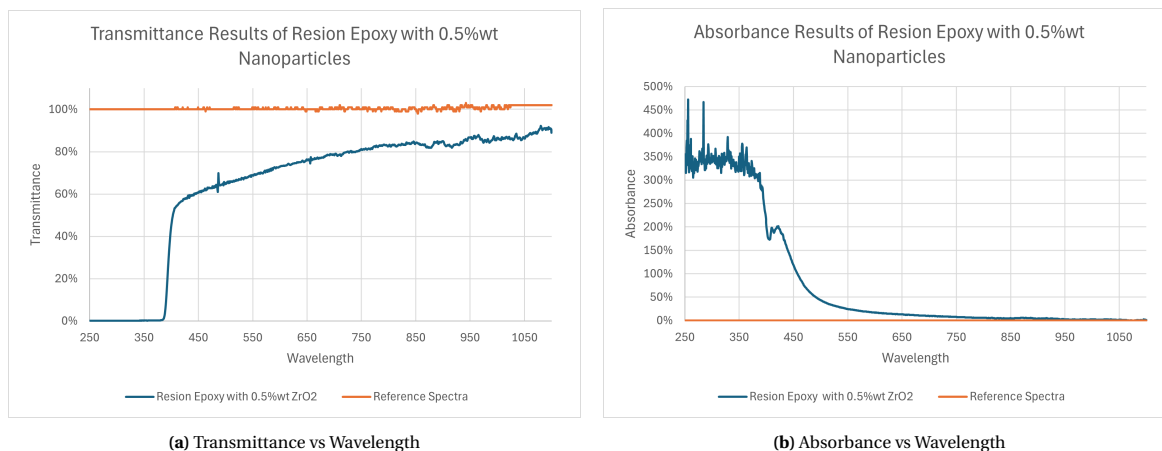


Figure A.7: Spectroscopy Test Results for PMMA Sample



## A.4 Individual Transmittance Results for Resins with Nanoparticles

Individual Transmittance Results for Resins with Nanoparticles.



**Figure A.8:** Spectroscopy Test Results for Resin Epoxy with 0.5%wt Nanoparticles

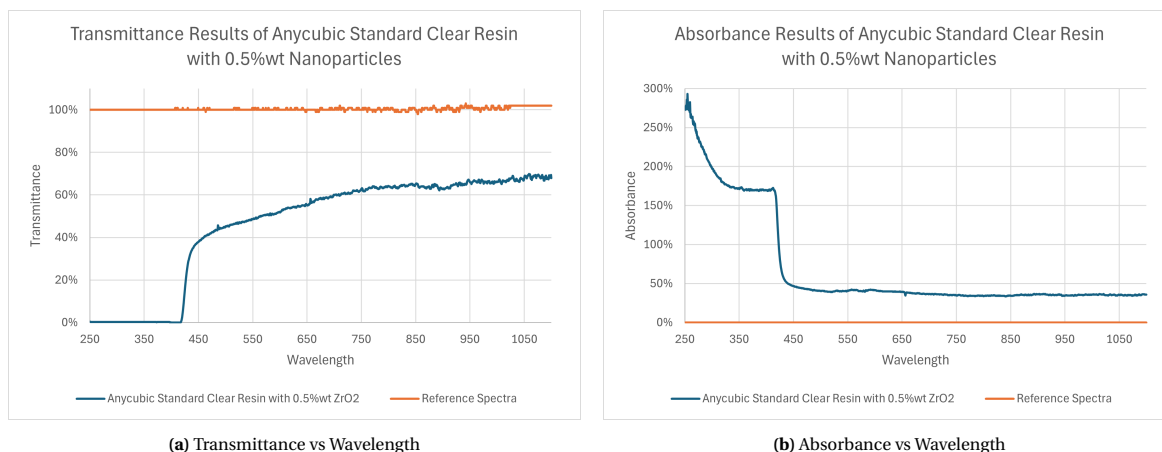


**Figure A.9:** Spectroscopy Test Results for Anycubic Standard Clear Resin with 0.5%wt Nanoparticles

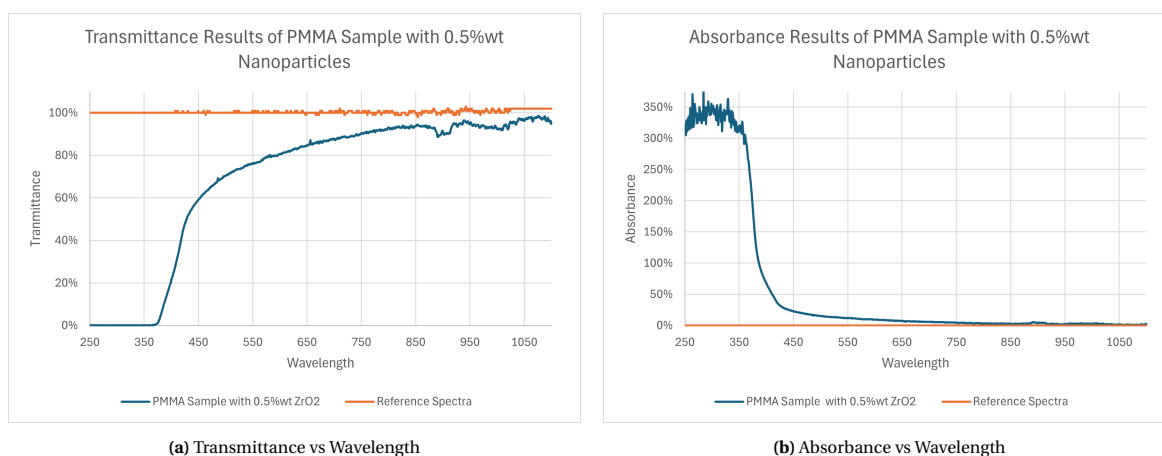


**Figure A.10:** Spectroscopy Test Results for PMMA Sample with 0.5%wt Nanoparticles

## A.5 Transmittance and Absorbance Results in NIR Region for Resins with 0%wt ZrO<sub>2</sub> Nanoparticles

Transmittance and Absorbance Results in NIR Region for Resins with 0%wt ZrO<sub>2</sub> Nanoparticles.

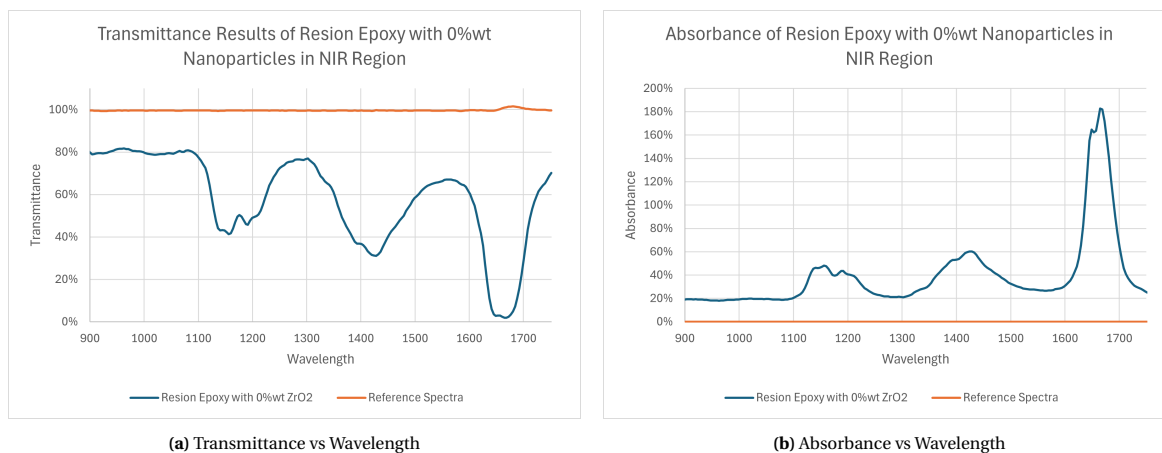


**Figure A.11:** Spectroscopy Test Results for Resion Epoxy Sample with 0%wt Nanoparticles in NIR Region

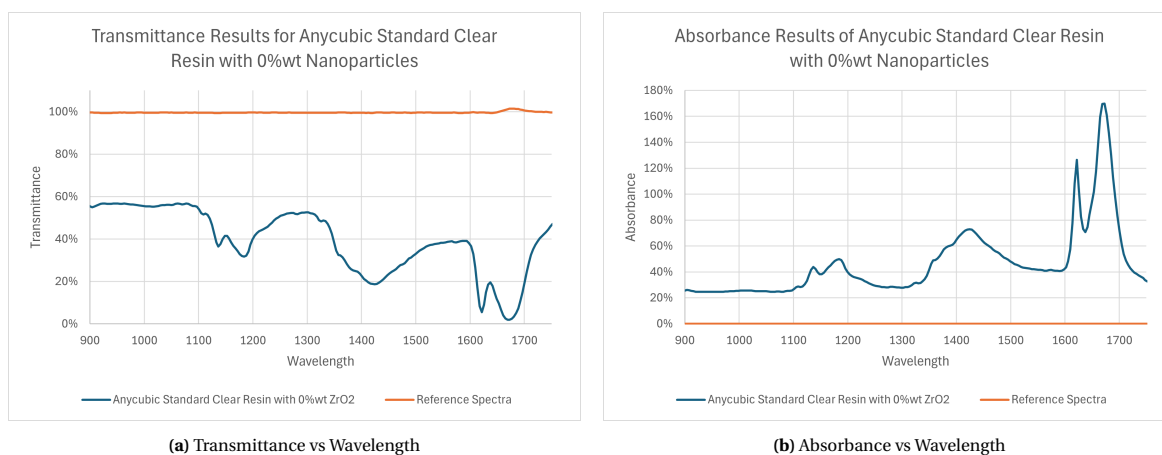


**Figure A.12:** Spectroscopy Test Results for Anycubic Standard Clear Resin Sample with 0%wt Nanoparticles in NIR Region

## A.6 Transmittance and Absorbance Results in NIR Region for Resins with 0.5%wt ZrO<sub>2</sub> Nanoparticles

Transmittance and Absorbance Results in NIR Region for Resins with 0.5%wt ZrO<sub>2</sub> Nanoparticles.

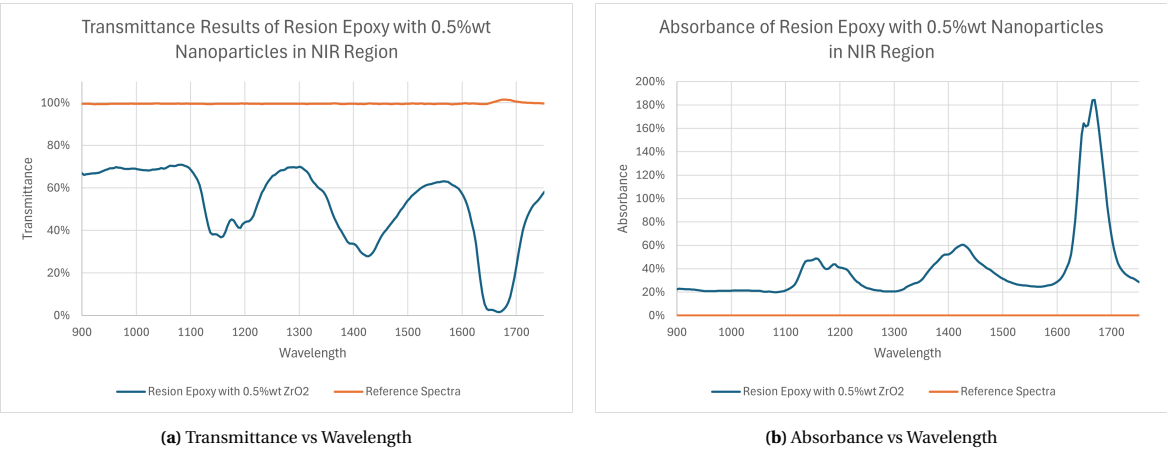


Figure A.13: Spectroscopy Test Results Resin Epoxy with 0.5%wt Nanoparticles in NIR Region

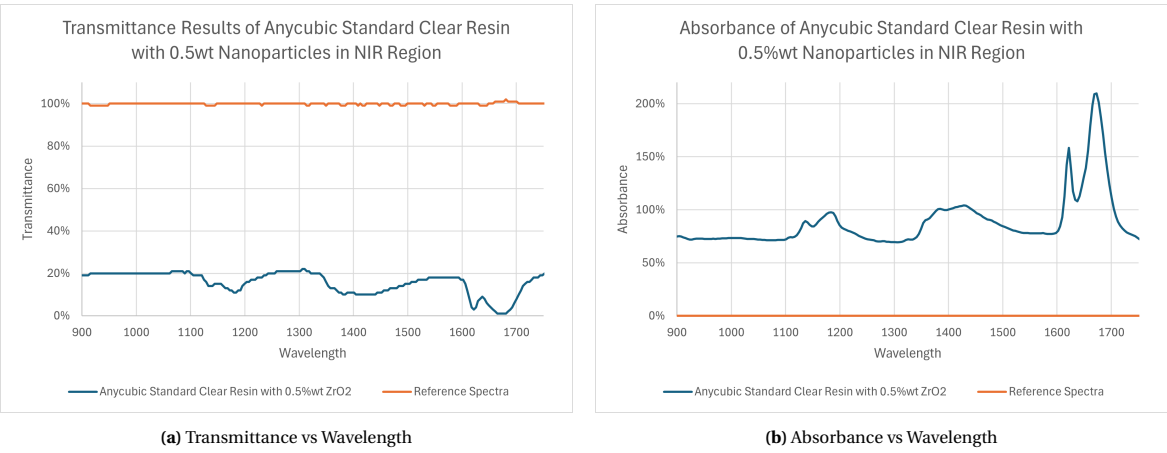


Figure A.14: Spectroscopy Test Results Anycubic Standard Clear Resin with 0.5%wt Nanoparticles in NIR Region

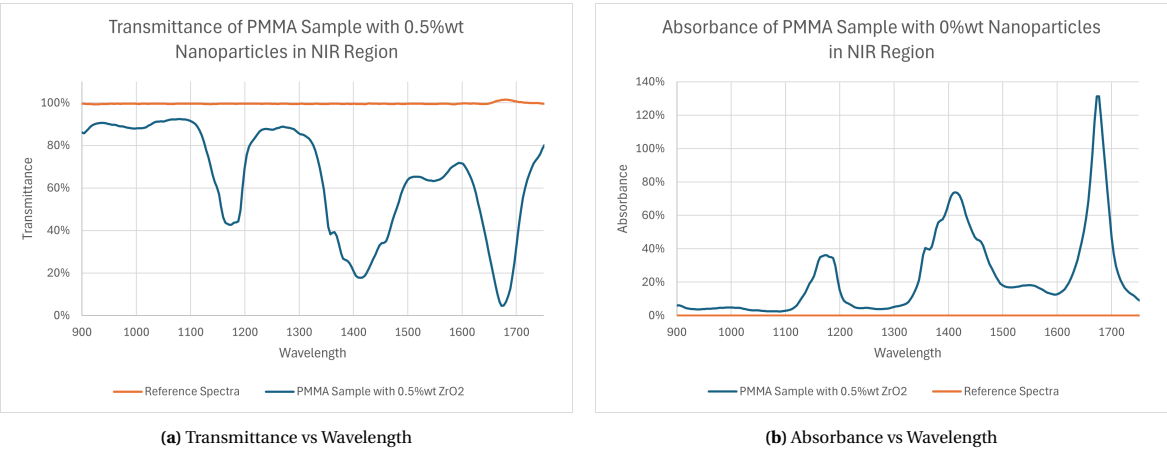
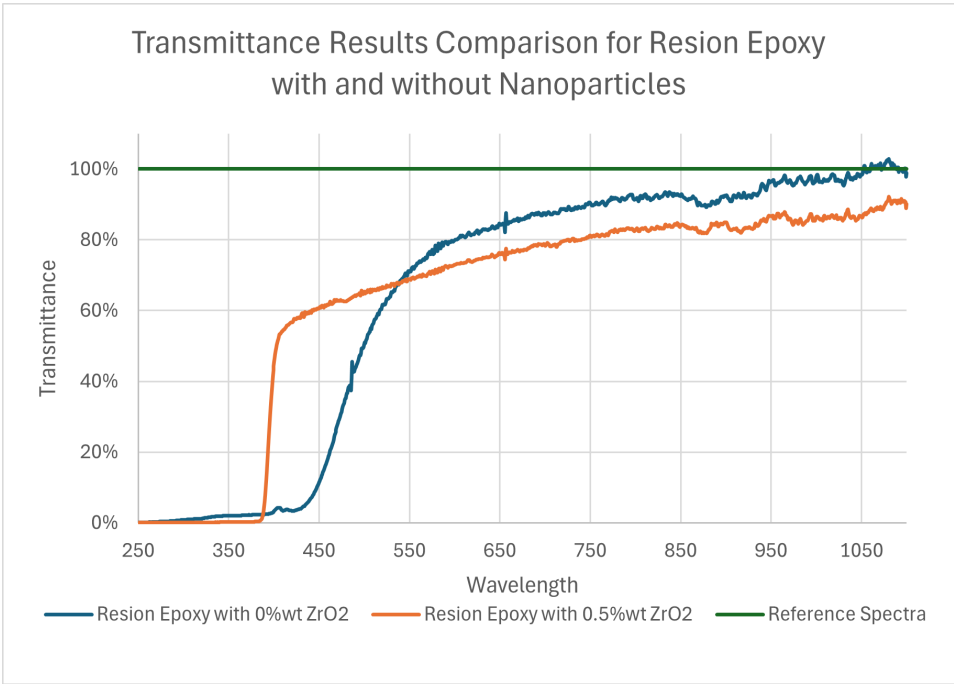


Figure A.15: Spectroscopy Test Results PMMA Sample with 0.5%wt Nanoparticles in NIR Region

A.6.1 Transmittance Comparison of Resins with and without Nanoparticles for Each Resin

Transmittance Comparison of Resins with and without Nanoparticles for Each Resin



**Figure A.16:** Transmittance comparison for Resion Epoxy Resin

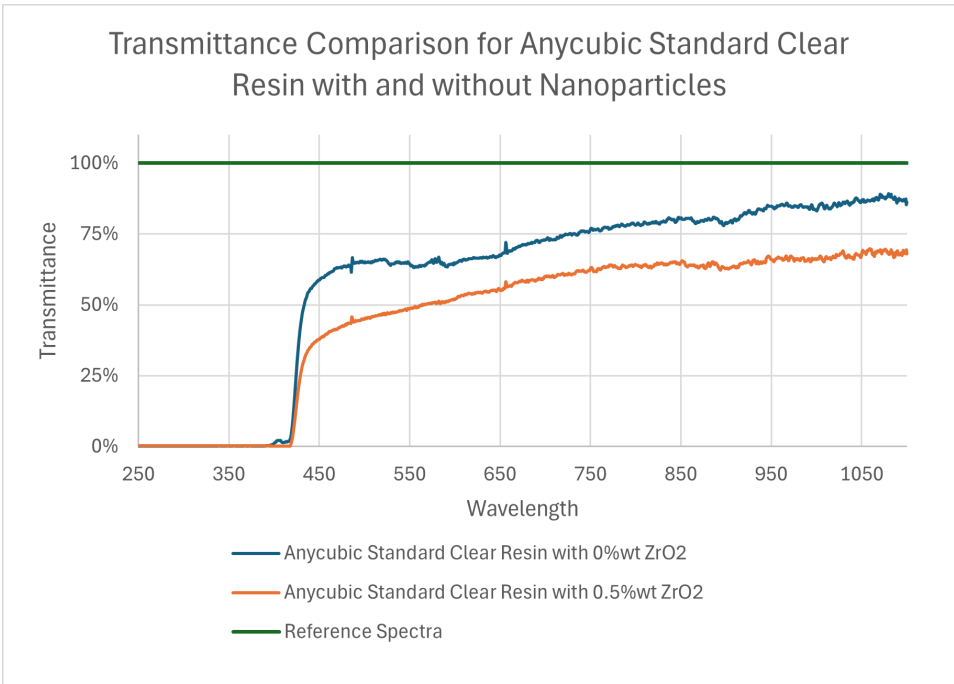


**Figure A.17:** Transmittance comparison for Anycubic Standard Clear Resin

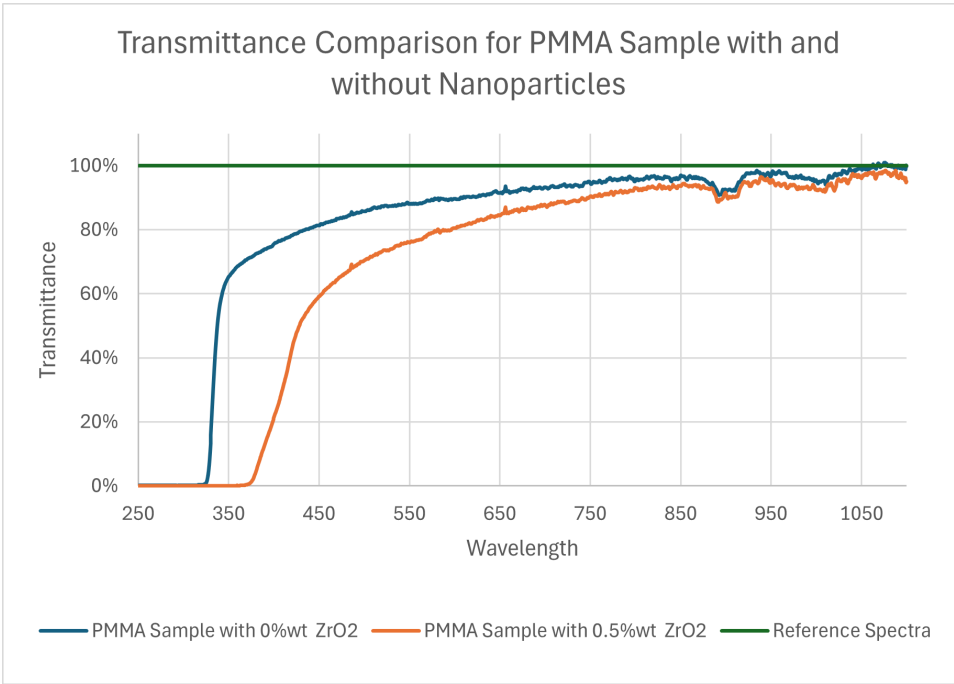


**Figure A.18:** Transmittance comparison for PMMA Sample

## A.7 Bill of Materials

Here is the bill of materials for the PCB components

Description	Supplier	Supplier Part Number	Amount	Price	Total Cost
JST SH 4-pin	Mouser	474-PRT-14417	3	€ 0.55	€ 1,65
Molex PicoClasp 12 pin	Mouser	538-501331-1207	3	€ 0.67	€ 2,01
Molex PicoClasp 8 pin	Mouser	538-501331-0807	3	€ 0.74	€ 2,22
Cui DC-DC converter	Mouser	490-P78E05-1000	3	€ 2.87	€ 8,61
Barreljack	Mouser	490-PJ-002B	3	€ 0.61	€ 1,83
Schottky Diode	Mouser	771-PMEG1020EJ-T/R	3	€ 0.251	€ 0,75
Raspberry Pi header Male	Kiwi Electronics	KW-2639	3	€ 1.95	€ 5,85
Raspberry Pi header female	Kiwi Electronics	KW-1650	3	€ 1.50	€ 4,50
100uF capacitor	Mouser	667-EEE-FN1E101UP	3	€ 0.47	€ 1,41
<b>Total</b>					<b>€ 28,83</b>

**Table A.5:** Bill of Materials